HHS Public Access

Author manuscript

Biochim Biophys Acta. Author manuscript; available in PMC 2018 March 01.

Published in final edited form as:

Biochim Biophys Acta. 2017 March ; 1862(3): 291–304. doi:10.1016/j.bbalip.2016.12.002.

Impact of Dietary Phytol on Lipid Metabolism in SCP2/SCPx/L-FABP Null Mice

Sherrelle Milligan[1], **Gregory G. Martin**[1], **Danilo Landrock**[1], **Avery L. McIntosh**[2], **John T. Mackie**[1], **Friedhelm Schroeder**[2], and **Ann B. Kier**[1]

[1]Department of Pathobiology, College of Veterinary Medicine & Biomedical Sciences, Texas A&M University, College Station, Texas, USA 77843-4467

[2]Department of Physiology/Pharmacology, College of Veterinary Medicine & Biomedical Sciences, Texas A&M University, College Station, Texas, USA 77843-4466

Abstract

In vitro studies suggest that liver fatty acid binding protein (L-FABP) and sterol carrier protein-2/sterol carrier protein-x (SCP2/SCPx) gene products facilitate uptake and metabolism and detoxification of dietary-derived phytol in mammals. However, concomitant upregulation of L-FABP in SCP2/SCPx null mice complicates interpretation of their physiological phenotype. Therefore, the impact of ablating both the L-FABP gene and SCP2/SCPx gene (L-FABP/SCP2/SCPx null or TKO) was examined in phytol-fed female wild-type (WT) and TKO mice. TKO increased hepatic total lipid accumulation, primarily phospholipid, by mechanisms involving increased hepatic levels of proteins in the phospholipid synthetic pathway. Concomitantly, TKO reduced expression of proteins in targeting fatty acids towards the triacylglycerol synthetic pathway. Increased hepatic lipid accumulation was not associated with any concomitant upregulation of membrane fatty acid transport/translocase proteins involved in fatty acid uptake (FATP2, FATP4, FATP5 or GOT) or cytosolic proteins involved in fatty acid intracellular targeting (ACBP). In addition, TKO exacerbated dietary phytol-induced whole body weight loss, especially lean tissue mass. Since individually ablating SCPx or SCP2/SCPx elicited concomitant upregulation of L-FABP, these findings with TKO mice help to resolve the contributions of SCP2/SCPx gene ablation on dietary phytol-induced whole body and hepatic lipid phenotype independent of concomitant upregulation of L-FABP.

Keywords

obesity; fatty acid; FABP; branched-fatty acid; phytol

Address Correspondence to: Ann B. Kier, Department of Pathobiology, Texas A&M University, TVMC, College Station, TX 77843-4467. Phone: (979) 862-1509, FAX: (979) 845-9231; akier@cvm.tamu.edu.

Disclosures: No conflicts of interest, financial, or otherwise, are declared by the authors.

Introduction

Much research has been directed towards exploring the effects of cytosolic lipid binding proteins on the metabolism of fatty acids, especially potentially toxic branched-chain fatty acids derived from dietary phytol. Phytol, a saturated sixteen-carbon chain-length fatty alcohol with four methyl branches, is released by ruminant bacterial cleavage of chlorophyll's side-chain for further conversion to branched-chain fatty acids [1]. While branched-chain fatty acids are often present at significant levels in meat and dairy products, serum levels are normally low, due to rapid hepatic uptake and metabolism [2-4]. However, in peroxisomal disorders of branched-chain fatty acid oxidation, serum and hepatic branched-chain fatty acid levels reach high toxic levels [2,3]. Branched-chain fatty acids such as phytanic acid have functional similarity to fibrates, hypolipidemic drugs used to treat cardiovascular disease, diabetes and metabolic syndrome [5,6]. Since branched-chain fatty acids are highly insoluble in aqueous, cytosolic lipid binding proteins have been proposed to act as ‘chaperones’ that facilitate their uptake, cytosolic transport, and targeting for degradation in oxidative organelles [7-11]. ‘Chaperones’ of particular interest are the protein products of the liver fatty acid binding protein (L-FABP) gene and of the sterol carrier protein-2/sterol carrier protein-x (SCP2/SCPx) gene.

While L-FABP has no enzymatic activity, it is quantitatively the most prevalent lipidic ligand ‘chaperone’ in liver cytosol [12-18]. L-FABP has high affinity for branched-chain lipids such as phytol-derived phytanic and pristanic acids [19,20], cholesterol [21], bile acids [22,23], and lipidic xenobiotics [24-26,26-31]. *In vitro* studies with cultured cells show that L-FABP enhances the uptake and peroxisomal oxidation of branched-chain fatty acids [7,9,10]. L-FABP has even been detected within peroxisomes, suggesting that it may not only chaperone bound branched-chain fatty acyl-CoA to peroxisomes but also to oxidative enzymes within peroxisomes [32].

SCP2 and SCPx, both encoded by the same SCP2/SCPx gene through alternate transcription sites, are also important contributors to branched-chain fatty acid metabolism [33]. Like L-FABP, SCP2 has no enzymatic activity, but binds branched-chain lipids such as phytol-derived phytanic and pristanic acids [19] and cholesterol [34]. SCP2 enhances branched-chain fatty acid cellular uptake and metabolism [8]. Hepatic SCP-2 concentration is about 6-8 fold less than that of L-FABP [13,35], with half in cytosol and the remainder primarily concentrated in peroxisomes [33,34,36]. Within the peroxisomal matrix, SCP2 directly interacts with fatty acid oxidative enzymes, suggesting a role in presenting bound branched-chain fatty acyl CoAs to these enzymes to facilitate their oxidation [37]. In contrast to SCP2 and L-FABP, SCPx is localized exclusively in peroxisomes [33,38,39]. SCPx functions as a ketothiolase enzyme with substrate specificity for both straight-chain and branched-chain fatty acids [38-42]. SCPx is the only known peroxisomal ketothiolase enzyme for β-oxidation of branched-chain fatty acids [41].

While gene ablation studies suggest physiological roles for both the L-FABP and SCP2/SCPx genes in branched-chain fatty acid uptake and metabolism, findings are complicated by concomitant upregulation of the non-ablated gene or genes. For example, individually ablating L-FABP [10,11], SCP2/SCPx [43-45], or SCPx [46] each impairs hepatic branched-

chain fatty acid uptake and/or metabolism. However, individually ablating SCP2/SCPx or SCPx concomitantly elicits marked upregulation of L-FABP [45-47]. Therefore, the current study examined the impact of ablating both the L-FABP and SCP2/SCPx genes on whole body and hepatic lipid phenotype of female mice fed a defined phytol diet.

Experimental Procedures

Materials

The Bradford protein micro-assay (Cat # 500-0001, bovine gamma globulin) was obtained from Bio-Rad (Hercules, CA). Diagnostic kits from Wako Chemicals (Richmond, VA) were used to measure triacylglycerol (L-type Triglyceride M, TG), free cholesterol (free cholesterol, C), total cholesterol (cholesterol E, TC), phospholipid (phospholipid, PL) and non-esterified fatty acid (HR Series NEFA-HR, NEFA). Diagnostic kits from Stanbio Laboratory (Boerne, TX) were used to determine β-hydroxybutyrate (β-Hydroxybutyrate LiquiColor, β-OHB), high density lipoprotein cholesterol (Direct HDL-Cholesterol, HDL-C), aspartate aminotransferase (Stanbio Alkaline Phosphatase LiquiColor, AST), and alanine aminotransferase (Stanbio Alanine Aminotransferase LiquiColor, ALT). Diagnostic kits from Diazyme Labs (Poway, CA) were used to measure apolipoprotein B (apoB), and apolipoprotein A-I (apoA1).

For hepatic mRNA quantitation, TaqMan® One-Step PCR Master Mix reagent kit and gene specific assays were purchased from Applied Biosystems (Foster City, CA) to determine hepatic expression of mouse glycerol-3-phosphate acyltransferase (GPAT) (*Gpam*; Mm00833328_m1), 1-acylglycerol-3-phosphate-O-acyltransferase (AGPAT) (*Agpat2*; Mm00458880_m1), Lipin (*Lpin2*; Mm00522390_m1), diacylglycerol acyltransferase (DGAT) (*Dgat2*; Mm00499536_m1), acetyl-coA carboxylase (ACC1) (*Acaca*; Mm01304285_m1), fatty acid synthase (FASN) (*Fasn*; Mm00662319_m1), 3-hydroxy-3-methylglutaryl-CoA (HMGCR) (*Hmgcr*; Mm01282492_m1), 3-hydroxy-3-methylglutaryl-CoA synthase (HMGCS1) (*Hmgcs1*, Mm01282492_m1), sodium-taurocholate cotransporting polypeptide (NTCP) (*Slc10*; Mm01302718_m1), organic anion-transporting polypeptide 1 (OATP1) (*Slco1*; Mm01267414_m1), organic anion-transporting polypeptide 2, OATP2 (*Slc22a7*; Mm00460672_m1), ATP-binding cassette sub-family G member 5 (ABCG5) (*Abcg5*; Mm01226965_m1) and ATP-binding cassette sub-family G member 8 (ABCG8) (*Abcg8*; Mm00445977_m1).

For western blotting of hepatic proteins, the following antibodies were obtained: Rabbit and goat polyclonal antibody to mouse acyl-CoA-binding protein (ACBP) (SC-23474, apoA1 (SC-23606), brain fatty acid binding protein (B-FABP) (SC-30088), bile salt export pump (BSEP) (SC-17294), carnitine palmitoyltransferase 1a (Cpt1a) (SC-31128), carnitine palmitoyltransferase 2 (Cpt2) (SC-20671), cellular retinoic acid binding protein 1 (CRABP I) (SC-10062), fatty acid transport protein 4 (FATP4) (SC-5834), farnesoid x receptor (FxR), glyceraldehyde 3-phosphate dehydrogenase (GADPH) (SC-13063), intestinal fatty acid binding protein (I-FABP) (SC-16063), LDL-Receptor (LDL-R) (SC-11826), liver x receptor (LxR) (SC-1201), multidrug resistance protein (MDR) (SC-8313), retinoid x receptor α (RxRα) (SC-553), sterol regulatory element-binding protein 1 (SREBP1) (SC-367) and sterol regulatory element binding protein 2 (SREBP2) (SC-8151) were obtained from Santa

Cruz Biotechnology (Dallas, TX). Rabbit and mouse polyclonal antibody to mouse acetyl-CoA acetyltransferase (ACAT2) (ab66259), apoB (ab31992), cytochrome c oxidase subunit IV (COX4) (ab16056), fatty acid transport protein 2 (FATP2) (ab83763) and fatty acid transport protein 5 (FATP5) (ab89008 were purchased from Abcam (Cambridge, MA). Sheep polyclonal antibody to bovine catalase (W90080C) was purchased from BioDesign (Dublin, OH). Rabbit polyclonal antibody to mouse glutamic oxaloacetic transaminase (GOT) (12248), LFABP (11294), p-thiolase (12464), SCP2 (12249), and SCPx (11306) were prepared as described [4,48]. Goat polyclonal antibody to mouse glutathione s-transferase (GST) (27457701V) was purchased from GE Life Sciences (Pittsburgh, PA). Bacterial polyclonal antibody to mouse 3alpha-hydroxysteroid reductase (3αHSD) (H9117-01) was purchased from US Biological (Peabody, MA). Rabbit polyclonal antibody to mouse PPARα (PA1-822A) was purchased from Pierce Antibody (Rockford, IL). Rabbit polyclonal antibody to mouse scavenger receptor class B member 1 (SR-B1) (NB400-104) was purchased from Novus Biological (Littleton, CO). Alkaline phosphatase-conjugated goat polyclonal antibody to rabbit IgG (product # A3687) as well as rabbit polyclonal antibody to goat IgG (product # A4187) was purchased from Sigma-Aldrich (St. Louis, MO). Alkaline phosphatase-conjugated rabbit polyclonal antibody to mouse IgG (product # ab6729-I) was obtained from Abcam (Cambridge, MA). Mouse monoclonal antibody to mouse GAPDH (MAB374) was purchased from Millipore (Billerica, MA). All reagents and solvents used were of the highest grade available.

Animals

Wild-type (WT) C57BL/6NCr mice were obtained from the National Cancer Institute (Frederick Cancer Research and Development Center, Frederick, MD). L-FABP/SCP-2/SCP-x null (TKO) mice were generated by our laboratory as previously described [49]. The term TKO is used since all three proteins encoded by the two genes (i.e. L-FABP as well as SCP-2 and SCP-x) were ablated. TKO mice were backcrossed >10 generations to the C57BL/6NCr background. Animals were housed in controlled conditions (T = 25 °C, H= 60-70% added humidity) under a 12:12 h light/dark cycle. All animal use protocols were approved by the Texas A&M Institutional Animal Care and Use Committee in compliance with the Guide for the Care and Use of Laboratory Animals. Animals were monitored for disease or injury daily as well as sentinel monitored quarterly, and were confirmed free of all known rodent pathogens.

Dietary phytol

One week before the study, all mice were moved from a standard pelleted rodent chow to a modified AIN-76A phytol-free, phytoestrogen-free pelleted control diet (5% calories from fat, diet no. D11243, Research Diets, New Brunswick, NJ). The control diet was used to minimize potential complications due to phytoestrogens [50,51] or phytol metabolites (e.g. phytanic acid), known to be the most potent naturally-occurring fatty acid ligand inducers of PPARα [20,52,53]. After one week, test mice were transferred to a modified AIN-76A pelleted rodent diet supplemented with 0.5% phytol (5% calories from fat, diet no. D01020601, Research Diets, New Brunswick, NJ), which is approximately ten times the total amount of free phytol and phytanic acid on average available in commercial laboratory rodent diets [6]. Two feeding groups contained 8 animals fed *ad libitum*: (a) WT mice fed

the 0.5% phytol diet, and (b) TKO mice fed the 0.5% phytol diet. The study was conducted for seven days because TKO mice exhibited a low tolerance for the 0.5% phytol diet, which manifested as a 20% percent loss in body weight. Body weight and food intake were measured every other day.

Whole body phenotype analysis and animal euthanasia

PIXImus images were taken of representative mice in the beginning (day 0) as well as all mice at the end of the study (day 8) as previously described [54]. Animals were anesthetized with a ketamine/xylazine mixture (0.01 mL/g body weight; 10 mg ketamine/mL and 1 mg xylazine/mL in 0.9% saline solution). Dual-energy X-ray absorptiometry (DEXA) using a Lunar PIXImus densitometer (Lunar Corp., Madison, WI) was performed as previously described [4] after calibration using a phantom mouse with known bone mineral density and fat tissue mass as described [4,55]. To obtain an *in vivo* measurement of whole body fat tissue mass (FTM) and bone-free lean tissue mass (LTM), the entire mouse, minus the head region, was exposed to sequential beams of high- and low-energy X-rays and an image was taken of the X-rays impacting a luminescent panel. Bone mass was differentiated from soft tissue mass by measuring the ratios of attenuation at different energies. The soft tissue mass was then separated into FTM and LTM as previously described [4]. At the end of the study, blood was collected via cardiac puncture followed by cervical dislocation as the secondary form of euthanasia according to the AVMA Guidelines for the Euthanasia of Animals. Blood was processed to serum and stored at −80 °C for subsequent lipid and protein analysis, and final DEXA images were taken.

Liver collection and analysis

After euthanasia, livers were harvested, weighed, snap frozen with dry ice, and stored at −80°C for lipid analysis, western blotting and reverse transcriptase-PCR analysis. Liver samples (~0.1 gram) were extensively minced, 0.5 mL PBS (pH 7.4) added, and homogenized using a motor-driven pestle (Tekmar Co, Cincinnati, OH) operating at 2000 rpm. Liver homogenate protein concentration was evaluated using the Bradford protein micro-assay (Bio-rad, Hercules, CA) in accordance with the manufacturer's instructions using Costar 96-well assay plates (Corning, Corning, NY) and the BioTek Synergy 2 micro-plate reader (BioTek Instruments, Winooski, VT). Liver homogenate lipids were measured using two different techniques. First, liver homogenate (5mg protein), as well as appropriate lipid standards (C, CE, TG, NEFA, and PL) were solvent-extracted and analyzed by thin layer chromatography (TLC) as described [17]. Second, liver homogenate lipids were quantified using Wako diagnostic kits in accordance with the manufacturer's instructions. To support the use of 96-well plates and the BioTek Synergy 2 micro-plate reader in measuring the liver lipids, sample/reagent volumes were adjusted accordingly. There was no significant difference in quatitative lipid measurements when comparing the two lipid analysis procedures described above. To determine cholesteryl ester concentration (CE), free (non-esterified) cholesterol concentration was subtracted from the total concentration. No significant differences were recognized between the solvent/extraction technique/TLC procedure and the diagnostic kit procedure.

Liver Histopathology and Serum Markers of Liver Toxicity

At the time of liver collection, liver slices were taken near the *porta hepatis*, fixed for 24 h in 10% neutral buffered formalin, put into individual cassettes with 70% alcohol, processed and embedded in paraffin, sectioned (4-6 microns), and stained with hematoxylin and eosin for histological evaluation [4,6]. Serum was obtained after overnight blood coagulation at 4°C, followed by centrifugation at 14,000 rpm for 20 min at 4°C and removal of the serum fraction. Stanbio diagnostic kits (Boerne, TX) were used to determine serum levels of aspartate aminotransferase (AST), alanine aminotransferase (ALT), and β-beta-hydroxybutyrate (β-OHB).

Serum lipid and apolipoprotein analysis

Serum lipids [free cholesterol (FC), total cholesterol (TC), HDL-cholesterol (HDL-C)], apoA1 and apoB levels were determined using commercially available diagnostic kits in accordance with the manufacturer's instructions (see above). The assays were modified to support the use of 96-well plates and micro-plate reader as described above. Serum cholesteryl ester (CE) concentrations were calculated by subtraction of serum FC from serum TC. Serum non-HDL-C was calculated by subtracting serum HDL-C from serum TC.

Real-time qRT-PCR

Quantitative real-time reverse transcription polymerase chain reaction (qRT-PCR) was performed on total mRNA isolated from livers and purified using an RNeasy minikit (Quiagen, Valencia, CA) in accordance with the manufacturer's protocol. mRNA concentrations and quality were measured using the ND-1000 method (Nanodrop Technologies, Inc., Wilmington, DE) where a 260/280 ratio of 1.9-2.1 was accepted as mRNA of good quality. For qRT-PCR, expression patterns were assessed using TaqMan One Step PCR Master Mix Reagent Kit, gene-specific TaqMan PCR probes, and primers. mRNA expression was quantitated with an ABI PRISM 7000 Sequence Detection System (Applied Biosystems, Foster City, CA) and using the following thermal cycling conditions: 48 degrees C for 30 minutes, 95 degrees C for 10 minutes before the first cycle, 95 degrees C for 15 seconds and 60 degrees C for 1 minute, repeated 40 times. Before amplification, total mRNA was reverse transcribed in the first step of the thermal cycler protocol (48 degrees C for 10 minutes) using TaqMan one step chemistry. For specific probes and primers, Assay-on-Demand products for mouse glycerol-3-phosphate acyltransferase-1 (*Gpam*; Mm00833328_m1), acylglycerolphosphate acyltransferase-2 (*Agpat2*; Mm00458880_m1), Lipin-2 (*Lpin2*; Mm00522390_m1), diacylglycerol acyltransferase-2 (*Dgat*; Mm00499536_m1), ATP-binding cassette subfamily G member 5 (*Abcg5*; Mm01226965), ATP-binding cassette subfamily G member 8 (*Abcg8*; Mm00445977_m1), acetyl CoA carboxylase-1 (*Acc1*; Mm01304285_m1), acetyl CoA carboxylase-2, cholesteryl ester hydrolase/hormone-sensitive lipase (*Lipe/Ceh/Hsl*; Mm00495359_m1), fatty acid synthase (*Fasn*; Mm00662319_m1), HMC-CoA synthase (*Hmgcs1*, Mm01304569_ml), HMG-CoA reductase (*Hmgcr*; Mm01282492_ml), Na+-taurocholate cotransporting polypeptide (*Ntcp*/Slc10a1; Mm01302718) and organic anion transporting polypeptide 1 (*Oatp1a1/Slco1a1*; Mm01267414_m1), organic anion transporting polypeptide 2 (*Oatp2/Slco1c1*; Mm00460672_m1) were obtained from Applied Biosystems. Experiments were analyzed

with ABI Prism 7000 SDS software (Applied Biosystems) to resolve the threshold cycle (C_T) from each well. Cycle number and primer concentrations were optimized to ensure that the reactions were analyzed in the linear phase of amplification. To analyze qRT-PCR data, mRNA expression was normalized to 18S RNA (a housekeeping gene) as described [56] and made relative to the control mouse group (male WT mice on control diet) set to one for final calculations.

Western Blotting

Western blot analysis was performed as in [57] to determine protein levels of hepatic proteins involved in cholesterol synthesis and metabolism (ACAT2, SREBP1, SREBP2), cholesterol uptake (SR-B1, LDL-R), biliary bile acid transport (OATP1, OATP2, NTCP, BSEP, MRP2), detoxification of peroxidized lipids (GST), cholesterol oxidation to bile acid (3αHSD, LXR1), fatty acid transport (FATP5, FATP2, FATP4, GOT, LFABP, IFABP, BFABP, ACBP, SCP2, CRABP I), fatty acid synthesis and oxidation (CPT1, CPT2, catalase, p-thiolase, 58 SCPX, 43 SCPX), and cholesterol transport to bile (PPARα, RXRα). Because each protein of interest and the housekeeping proteins COX4 and GADPH were easily determined by size on the tricene gels, membrane blots were cut into two. This was so that each western blot was probed with antisera against the protein of choice and against COX4 or GADPH to ensure uniform protein loading. Protein bands were visualized with alkaline-phosphatase conjugated goat anti-rabbit or mouse IgG and Sigma Fast 5-bromo-4-chloro-3-indolyn phosphate/nitroblue tetrazolium tablets (Sigma Chemical Co, St. Louis, MO). To quantitate protein levels in the blots images were obtained using single-chip CCD video camera and a computer workstation (IS-500 system, Alpha Innotech, San Leandro, CA). Image proteins (mean 8-bit grayscale density) were quantitated by densitometric analysis using NIH Image (available by anonymous FTP). Expression of each protein was normalized to the mean expression of COX4 or GAPDH. Linear standard curves were produced from Western blots where pure protein (L-FABP, SCP2, ACBP) was available for quantitative analysis. Band intensities on western blots were analyzed as described above and then plotted against the protein amount to produce a standard curve within the linear range of each protein. Changes in protein expression between liver homogenate samples were measured by comparing the sample with the standard curve on each blot. Proteins with no source of pure protein were expressed as relative fold differences between samples as described [46].

Statistics

Each feeding group contained 8 animals. All values were expressed as averages ± standard error of the mean (SEM) with n and p values indicated in figure legends. Statistical analysis was performed using t-test (GraphPad Prism, San Diego, CA, San Jose, CA). Values with $p < 0.05$ were considered statistically significant.

Results

Body Weight, Liver Weight, Liver Histopathology and Serum AST and ALT

Dietary phytol significantly decreased weight gain in WT mice, an effect exacerbated by TKO (Fig 1A). The phytol-induced weight loss was attributable to both reduced food

consumption and reduced energy intake. Phytol decreased food consumption by 16±3% in WT and nearly twice as much by 29±2% in TKO mice (not shown). This suggested that TKO exacerbated the effect of dietary phytol on weight loss by decreasing food intake.

Dietary phytol was associated with mild hepatocellular necrosis in both WT and TKO (not shown) with no difference between the phytol fed mouse groups in liver weight/body weight ratio or liver weight (Fig 1B,C). These observations were supported by measurement of serum values of ALT and AST, other indicators of hepatocyte damage. Although dietary phytol increase ALT and AST values similarly in both WT and TKO mice, all values were within the normal range of mouse serum ALT and AST values (less than 150 and 330 units/l, respectively) shown for blood chemistry and hematology in 8 inbred strains of mice, MPD: Eumorphia. Mouse Phenome Database web site, The Jackson Laboratory, Bar Harbor, Maine USA. http://phenome.jax.org [Cited 29 Oct, 2014] (Fig 1D,E). Taken together, these measures indicated that the major changes in whole body and liver lipid phenotype elicited by TKO in phytol fed mice detailed in the following sections were not due to marked hepatotoxicity.

Body Composition: Fat Tissue Mass and Lean Tissue Mass

PIXImus dual-energy x-ray absorptiometry (DEXA) scans were done to determine if any decline in weight gain, was due to selective loss of fat or protein. Representative PIXImus images of mice from the beginning (Fig 2A,B) and end (Fig. 2C,D) of the dietary study suggested gross differences in body composition. Phytol-fed WT mice appeared visually smaller at the end of the study (Fig 2A,C). This difference appeared even more marked in phytol-fed TKO mice (Fig 2B,C). DEXA analysis of multiple mice to resolve FTM (Fig 2E) and LTM (Fig 2F) showed that dietary phytol increased FTM while concomitantly decreasing LTM (Fig 2E,F). In contrast, TKO decreased both FTM and LTM (Fig. 2E,F).

Hepatic Lipid and Glyceride Accumulation

Total hepatic lipid was markedly higher in phytol-fed TKO mice than phytol-fed WT mice, both when expressed on the basis of nmol/mg liver protein (Fig 3A) or when expressed on the basis of nmol/mg liver wet weight (Supplementary Fig. 3A). This change was attributed primarily to a decrease in neutral lipid, expressed both on the basis of nmol/mg liver protein (Fig 3B) or when expressed on the basis of nmol/mg liver wet weight (Supplementary Fig. 3B). It was also due in part to the nearly 3-fold increase in phospholipid expressed both on the basis of nmol/mg liver protein (Fig 3C) or when expressed on the basis of nmol/mg liver wet weight (Supplementary Fig. 3C). In contrast, triacylglycerol actually decreased about 25% when expressed both on the basis of nmol/mg liver protein (Fig 3D) or when expressed on the basis of nmol/mg liver wet weight (Supplementary Fig. 3D). Hepatic phospholipid accumulation was associated with a more than two-fold increase in expression of the key enzymes in the synthesis of phosphatidic acid (precursor of both phospholipids and triacylglycerols), i.e. *Gpam* (Fig 3E) and *Agpat* (Fig 3F) and despite no change in SREBP1 (Fig 4A), increased expression of *Acc1*, the rate limiting enzyme in *de novo* fatty acid synthesis (Fig 4B). Though *Dgat* is a key enzyme in the synthesis of triacylglycerol and was significantly higher in TKO mice than WT mice (Fig 3H), this increase was not reflected in hepatic triacylglycerol levels. On the contrary, triacylglycerol levels were significantly less

in TKO mice. This decrease correlated with decreased expression of *Fasn*, a key enzyme in fatty acid synthesis (Fig 4C), and increased expression of *Lipe*, a key enzyme in triacyglycerol hydrolysis (4G). However it is equally plausible that phytol toxicity caused decreases in triacyglycerol and *Fasn* expression independently. Taken together, these findings suggested that the TKO induced hepatic lipid accumulation by favoring fatty acyl targeting towards phospholipids at the expense of triacylglycerol in phytol-fed TKO phytol-fed mice.

Hepatic Fatty Acid Oxidation

Hepatic glyceride accumulation in phytol-fed TKO mice may arise not only from increased *de novo* lipogenesis, but also from increased uptake and/or decreased oxidation of fatty acids.

While loss of L-FABP and SCP-2, both facilitators of fatty acid uptake, was expected to increase serum non-esterified fatty acid (NEFA) level, on the contrary TKO did not significantly changes serum NEFA (Fig 5A). This lack of increase in serum NEFA was attributable in part to concomitant downregulation of hepatic membrane fatty acid transporter FATP5 (Fig 5B) (FATP2 and FATP4, Fig 5C,D, remained unchanged) and downregulation of GOT (Fig 5E).

TKO did not decrease serum (Fig 6A) or hepatic (Fig 6B) levels of β-hydroxybutyrate (β-OHB), a measure of hepatic fatty acid oxidation. This was reflected in no change in the levels of hepatic expression of key enzymes in mitochondrial (CPT1A, CPT2) fatty acid β-oxidation (Fig. 6C,D) or peroxisomal fatty acid β-oxidation (Fig 6 E,F). As expected, the other major enzymes in peroxisomal fatty acid β-oxidation, i.e. SCPx (58kDa) and SCPx (43kDa), were not detectable in these TKO mice (Fig 6G,H). In addition, there was no significant change in the expression of nuclear receptors regulating transcription of fatty acid β-oxidative enzymes (Fig 6I,J).

Thus, the TKO-induced increase in hepatic glycerides was not associated with either increased expression of membrane transport proteins involved in fatty acid uptake or a decrease in fatty acid β-oxidation. Instead, the TKO-induced increase in hepatic glyceride was associated with increased fatty acid synthesis, represented by an increase in key enzymes, particularly an increase in *Acc1*, the rate limiting enzyme in fatty acid synthesis (Fig 4B).

Hepatic Cholesterol Accumulation

Despite there being no change in SREBP2, which plays a major role in cholesterol homeostasis (Fig 4D), the finding that TKO increased total neutral lipid, despite decreasing triacylglycerol, suggested upregulation of the other major neutral lipid species, cholesterol and/or cholesteryl ester perhaps as a result of the upregulated expression of target genes in cholesterol synthesis (*Hmgcs1*, *Hmgcr*) (Fig 4E,F). However, there was no effect on hepatic total cholesterol, free cholesterol or cholesteryl ester levels (Fig 7A-C) nor was there a change in the expression of the cholesteryl ester synthetic enzyme (acyl CoA cholesterol acyltransferase, ACAT 2) (Fig 7D). In contrast, there was marked upregulation of hepatic expression of the *Lipe* gene, which codes for the degradative enzyme cholesteryl ester

hydrolase (CEH) (Fig 4G). Thus, upregulation of *Lipe* did not actively decrease hepatic cholesterol levels in phytol-fed TKO.

Serum Levels of Cholesterol and Lipoproteins in Serum Cholesterol Transport

In phytol-fed mice, TKO significantly increased both serum cholesterol and cholesterol ester, regardless whether data were expressed on the basis of nmol lipid/ml serum (Fig 8A,B) or nmol lipid/mg serum protein (Supplementary Fig. 2A,B). With no changes in HDL-C, lipoprotein rich in apoA1 or apoA1/HDL ratio (Fig 8 C,D,E), this increase is attributed to increased lipoprotein rich in apoB as well as increased non-HDL-C (Fig. 8F, G) in the serum. However, these increases in serum cholesterol did not correlate with any change in hepatic accumulation of cholesterol (Fig. 7A-C). These findings suggest that TKO, in combination with phytol, has a “protective” effect against hepatic cholesterol accumulation.

Hepatic Expression of Proteins Involved in Cholesterol Basolateral Uptake/Efflux and Canalicular Secretion

TKO and dietary phytol differentially impacted hepatic expression of proteins involved in hepatic cholesterol uptake and loss.

TKO did not alter hepatic levels of scavenger receptor B1 (SR-B1) or low density lipoprotein receptor (LDL-R), the key receptors in bidirectional uptake/efflux of high density lipoprotein (HDL) cholesterol and low density lipoprotein (LDL) cholesterol (Fig 9C, D), or apoA1, involved in hepatic cholesterol secretion to nascent-HDL (Fig 9A) at the basolateral membrane. In contrast, TKO markedly decreased hepatic accumulation of apoB, the key apoprotein in LDL (Fig 9B). Concomitantly, TKO did not affect expression of ATP binding cassette proteins localized in the canalicular membrane for transporting hepatic cholesterol into bile, i.e. *Abcg5*, *Abcg8* (Fig 9E,F). Low level of apoB in the liver was reflected by high levels of apoB in the serum in TKO mice.

Bile Acid and Transport

Since bile acid level in large part drives biliary cholesterol secretion [58-60], hepatic expression of proteins involved in bile acid reuptake from serum (*Oatp1, Oatp2, Ntcp*), bile acid cytosolic transport (L-FABP, SCP2, 3αHSD, GST), and biliary secretion of bile acid (BSEP) and phospholipid (MDR) at the canalicular membrane was examined.

With regards to basolateral proteins in bile acid uptake from serum, TKO significantly decreased hepatic expression of *Oatp1* (Fig 10A), but increased that of *Oatp2* (Fig 10B) and *Ntcp* (Fig 10A,C). TKO decreased expression of the nuclear regulatory protein FxR, but did not affect the nuclear regulatory protein LxR (Fig 10H,I). These proteins are responsible for regulating transcription of target genes in bile acid metabolism and uptake.

Regarding cytosolic bile acid binding/transport proteins, TKO abolished expression of the major murine cytosolic bile acid binding/transport protein L-FABP (Fig 11A), and this null effect was not compensated for by upregulation of the other known cytosolic bile acid binding/transport proteins (3αHSD, GST, Fig 10D-E).

With regards to canalicular membrane proteins involved in hepatic bile acid export into bile, TKO did not affect expression of the bile salt export protein BSEP (Fig 10H) or the canalicular membrane protein for phospholipid transport into bile (MDR, Fig 10G).

Other Fatty Acid Binding and Transport Proteins

The possibility of potential compensatory upregulation of other fatty acid and cholesterol binding proteins occurred in response to loss of L-FABP and SCP2/SCPx (TKO) was examined. As expected, TKO alone resulted in complete loss of L-FABP (Fig 11A) as well as all SCP2/SCPx gene products, SCP2 (Fig 11B), SCPx (58kDa) (Fig 6G), and SCPx (43kDa) (Fig 6H). These ablations resulted in compensatory upregulation of other known FABP family members including I-FABP (Fig 11D) and A-FABP (Fig 11F) with no compensatory upregulation of B-FABP (Fig 11E) or CRABP1 (Fig 11G).

Discussion

Since accumulation of branched-chain fatty acids derived from dietary phytol is toxic [2,3], most research has focused on identification of the individual peroxisomal enzymes in their metabolism and the pathological consequences of genetic mutations therein [61-65]. In contrast, much less is known about how these poorly soluble branched-chain lipids traffic through the hepatocyte cytosol for metabolism. *In vitro* ligand binding [7,9,10,19] and transfected cell [7-10] studies suggest L-FABP and SCP2/SCPx gene products act as their potential ‘chaperones’. Further, a highly prevalent human L-FABP SNP (26-38% allele frequency) [66-72] resulting in L-FABP T94A substitution alters uptake/metabolism of another branched-chain lipid, cholesterol [29,67,71,73]. Human subjects expressing the L-FABP T94A variant exhibit marked triglyceride accumulation in liver [29,71], elevated triglyceride and LDL cholesterol in serum [67,74,75], and increased incidence of cardiovascular disease [67,69,74]. Although less prevalent, a mutation in the human SCP-x gene completely abolishes SCP-x activity, markedly elevates serum levels of branched chain fatty acids (phytanic acid, pristanic acid), and induces neurodegeneration [76,77]. While gene-targeted mice ablated in L-FABP [10,11,78-84], SCPx [46], or SCP2/SCPx [5,44,45,47,85] have proven useful in resolving respective physiological roles, concomitant upregulation of the non-ablated chaperone, especially L-FABP in SCP2/SCPx null or SCPx null mice, complicates interpretation of phenotype [45-47]. The current study with mice ablated in both SCP2/SCPx and L-FABP genes (SCP2/SCPx/L-FABP triple gene ablation or TKO) provided several important insights:

First, ablating both L-FABP and SCP2/SCPx significantly affected whole body phenotype in mice fed a high phytol diet as compared to ablating each individually. In earlier findings, feeding dietary phytol alone decreased body weight of female wild-type (WT) mice [6], an effect not further exacerbated upon ablating L-FABP [11]. In contrast, singly ablating SCPx or SCP2-SCPx markedly exacerbated phytol diet-induced weight loss several-fold [45,46]. Likewise, ablating L-FABP in SCP2/SCP-x null mice (i.e. TKO) nearly doubled the dietary phytol-induced weight loss, an effect attributed to decreased food consumption.. These data indicated that concomitant upregulation of L-FABP in SCP2/SCPx null or SCPx null mice [45-47,57] did not diminished and/or obscure the impact of SCP2/SCPx ablation on dietary

phytol-induced weight loss. This suggested that SCP2/SCPx may play a greater role than L-FABP in exacerbating phytol-induced weight loss.

Second, the TKO data presented herein suggested that SCP2/SCPx gene products, much more than the L-FABP, contributed to phytol oxidation. In response to dietary phytol, peroxisomal oxidation products of phytanic acid and pristanic acid accumulate concomitant with upregulation of L-FABP, SCP2, SCP-x and peroxisomal oxidative enzymes in WT mice [6]. L-FABP gene ablation did not further exacerbate this dietary phytol-induced increase likely due to concomitant upregulation of SCP-x, a key peroxisomal enzyme in phytol oxidation [11]. In contrast, singly ablating SCPx or SCP2-SCPx markedly decreased dietary phytol-induced accumulation of phytol metabolites despite concomitant upregulation of L-FABP [45-47,57] and some fatty acid oxidative enzymes [45,46]. Ablating L-FABP in SCP2/SCP-x null mice (i.e. TKO) did not further exacerbate dietary-phytol induced oxidation and upregulation of fatty acid oxidative enzymes. These findings suggested that SCP2/SCPx gene products may play a greater role in phytol oxidation than L-FABP. Consistent with this possibility, nearly half of SCP2 is peroxisomal, while all of SCPx is peroxisomal and SCPx is the only known peroxisomal ketoacyl-CoA thiolase involved in branched chain fatty acid oxidation [33]. Despite these findings, however, L-FABP may serve a lesser role in phytol metabolism, i.e. in re-uptake of excess phytol metabolites from serum [10]. L-FABP enhances fatty acid uptake [86-88], accounts for 80-90% of hepatic cytosol binding/transport capacity for fatty acids and fatty acyl-CoAs [17,18], and is the most prevalent cytosolic transporter for targeting these ligands to mitochondria and peroxisomes for oxidation [85,89,90]. Loss of L-FABP alone decreases hepatocyte uptake of phytanic acid [10]. In contrast, ablation of SCP2/SCPx significantly decreases serum NEFA, attributable in large part to marked upregulation of L-FABP [45,57]. TKO offset the effect of L-FABP upregulation in SCP2/SCPx ablated mice since serum NEFA levels were unaltered. Taken together, these findings suggested that in the context of high dietary phytol, SCP2/SCPx has a greater role in oxidation while L-FABP may have a role in reuptake.

Third, TKO markedly increased hepatic lipid accumulation, primarily due to increased phospholipid, in phytol-fed female mice. Earlier it was shown that dietary phytol alone increased hepatic lipid accumulation, primarily by increasing phospholipid in female wild-type (WT) mice [6], an effect exacerbated upon L-FABP ablation [11]. L-FABP is known to stimulate the rate limiting enzyme in phospholipid synthesis (GPAT) *in vitro* [91-93]. L-FABP overexpression in transfected cells increases fatty acid uptake and incorporation into triglyceride, albeit quantitatively not as much as into phospholipid [86]. In contrast, singly ablating SCPx or SCP2-SCPx decreased hepatic total lipid, primarily by decreasing triglyceride [45,46] concomitant with upregulation of L-FABP [45-47,57]. Ablating L-FABP in SCP2/SCPx mice (i.e. TKO) fed phytol mice reflected a combined phenotype where phospholipid was increased nearly 5-fold at the expense of triglyceride. The increased hepatic phospholipid was associated with increased transcription of the rate limiting gene in *de novo* fatty acid synthesis (*Acc1*) and enzymes in phospholipid synthesis (*Gpam*, *Agpa*t). Taken together, these findings suggested that in the context of phytol-diet, L-FABP and SCP2/SCPx play somewhat different roles in hepatic lipid accumulation, differing in preferentially impacting phospholipid vs triglyceride.

Fourth, phytol diet TKO increased cholesterol in the serum, but not liver. Dietary phytol alone did not alter hepatic cholesterol accumulation in female wild-type (WT) mice [11]. However, L-FABP gene ablation significantly increased only hepatic free cholesterol, but not cholesteryl ester or total cholesterol, in phytol-fed females [11]. Likewise, singly ablating SCPx did not significantly alter hepatic total, free, or esterified cholesterol in female mice [46] while ablating SCP2/SCPx increased hepatic total and esterified cholesterol level [57] —effects likely attributed to concomitant greater upregulation of L-FABP [45-47,57]. L-FABP overexpression in cultured cells enhances cholesterol uptake and intracellular targeting for esterification [94,95]. Concomitant L-FABP upregulation in SCP2 overexpression mice also induces hepatic cholesterol accumulation [96-98]. Taken together, these data suggested that L-FABP upregulation may counteract the effect of ablating SCP2/SCPx or SCPx on hepatic cholesterol.

In summary, the results presented herein with TKO mice shed significant new insights into the roles of L-FABP and SCP2/SCPx genes in whole body weight gain and hepatic lipid metabolism in response to dietary phytol. TKO exacerbated dietary phytol-induced whole body weight loss, especially lean tissue mass (LTM). TKO also increased hepatic total lipid accumulation, primarily phospholipid, in response to upregulation of hepatic levels of proteins in the phospholipid synthesis. Increased hepatic lipid accumulation was not attributable to any concomitant upregulation of membrane fatty acid transport/translocase proteins involved in fatty acid uptake (FATP2, FATP4, FATP5 or GOT) or cytosolic proteins involved in fatty acid intracellular targeting (ACBP). Since individually ablating SCPx or SCP2/SCPx elicited concomitant upregulation of L-FABP, these findings with TKO mice significantly contribute to our understanding of the respective roles of these genes in dietary phytol metabolism.

Supplementary Material

Refer to Web version on PubMed Central for supplementary material.

Acknowledgments

We would like to acknowledge Kerstin Landrock, Huan Huang, Stephen Storey, and Kimberly Hein for their contribution to this work.

Grants: This work was supported by NIH grants RO1 DK41402 (FS, ABK), R25 OD016574 (SM, ABK), and T35 OD010991 (SM, ABK).

This work was supported by US Public Health Service/National Institutes of Health Grants RO1 DK41402 (FS, ABK), R25 OD 016574 (SM, ABK), and NIH T35 Veterinary Scholars Program, CVM (SM, ABK).

References

1. Steinberg, D. The Metabolic Basis of Inherited Disease. Scriver, CR.Beaudet, AL.Sly, WS., Valle, D., editors. McGraw-Hill; New York: 1990. p. 1533-1550.
2. Verhoeven NM, Jakobs C. Human metabolism of phytanic acid and pristanic acid. Prog Lipid Res. 2001; 40:453–466. [PubMed: 11591435]
3. Avigan J. The presence of phytanic acid in normal human and animal plasma. Biochim Biophys Acta. 1966; 166:391–394.

4. Atshaves BP, Payne HR, McIntosh AL, Tichy SE, Russell D, Kier AB, Schroeder F. Sexually dimorphic metabolism of branched chain lipids in C57BL/6J mice. J Lipid Res. 2004; 45:812–830. [PubMed: 14993239]
5. Kannenberg F, Ellinghaus P, Assmann G, Seedorf U. Aberrant oxidation of the cholesterol side chain in bile acid synthesis of sterol carrier protein-2/sterol carrier protein-x knockout mice. J Biol Chem. 1999; 274:35455–35460. [PubMed: 10585416]
6. Mackie JT, Atshaves BP, Payne HR, McIntosh AL, Schroeder F, Kier AB. Phytol-induced hepatotoxicity in mice. Toxicol Pathol. 2009; 37:201–208. [PubMed: 19188468]
7. Atshaves BP, Storey SM, Petrescu AD, Greenberg CC, Lyuksyutova OI, Smith R, Schroeder F. Expression of fatty acid binding proteins inhibits lipid accumulation and alters toxicity in L-cell fibroblasts. Am J Physiol. 2002; 283:C688–C703.
8. Atshaves BP, Storey SM, Schroeder F. Sterol carrier protein-2/sterol carrier protein-x expression differentially alters fatty acid metabolism in L-cell fibroblasts. J Lipid Res. 2003; 44:1751–1762. [PubMed: 12810824]
9. Atshaves BP, Storey S, Huang H, Schroeder F. Liver fatty acid binding protein expression enhances branched-chain fatty acid metabolism. Mol Cell Biochem. 2004; 259:115–129. [PubMed: 15124915]
10. Atshaves BP, McIntosh AL, Lyuksyutova OI, Zipfel WR, Webb WW, Schroeder F. Liver fatty acid binding protein gene ablation inhibits branched-chain fatty acid metabolism in cultured primary hepatocytes. J Biol Chem. 2004; 279:30954–30965. [PubMed: 15155724]
11. Atshaves BP, McIntosh AL, Payne HR, Mackie J, Kier AB, Schroeder F. Effect of branched-chain fatty acid on lipid dynamics in mice lacking liver fatty acid binding protein gene. Am J Physiol. 2005; 288:C543–C558.
12. McArthur MJ, Atshaves BP, Frolov A, Foxworth WD, Kier AB, Schroeder F. Cellular uptake and intracellular trafficking of long chain fatty acids. J Lipid Res. 1999; 40:1371–1383. [PubMed: 10428973]
13. Atshaves BP, Martin GG, Hostetler HA, McIntosh AL, Kier AB, Schroeder F. Liver fatty acid binding protein (L-FABP) and Dietary Obesity. Journal of Nutritional Biochemisty. 2010; 21:1015–1032.
14. Furuhashi M, Hotamisligil GS. Fatty acid binding proteins: role in metabolic diseases and potential as drug targets. Nature Reviews Drug Discovery. 2008; 7:489–503. [PubMed: 18511927]
15. Storch J, Thumser AE. The fatty acid transport functions of fatty acid binding proteins. Biochim Biophys Acta. 2000; 1486:28–44. [PubMed: 10856711]
16. Storch J, Corsico B. The emerging functions and mechanisms of mammalian fatty acid binding proteins. Annu Rev Nutr. 2008; 28:18.1–18.23.
17. Martin GG, Danneberg H, Kumar LS, Atshaves BP, Erol E, Bader M, Schroeder F, Binas B. Decreased liver fatty acid binding capacity and altered liver lipid distribution in mice lacking the liver fatty acid binding protein (L-FABP) gene. J Biol Chem. 2003; 278:21429–21438. [PubMed: 12670956]
18. Martin GG, Huang H, Atshaves BP, Binas B, Schroeder F. Ablation of the liver fatty acid binding protein gene decreases fatty acyl CoA binding capacity and alters fatty acyl CoA pool distribution in mouse liver. Biochem. 2003; 42:11520–11532. [PubMed: 14516204]
19. Frolov A, Miller K, Billheimer JT, Cho TC, Schroeder F. Lipid specificity and location of the sterol carrier protein-2 fatty acid binding site: A fluorescence displacement and energy transfer study. Lipids. 1997; 32:1201–1209. [PubMed: 9397406]
20. Wolfrum C, Ellinghaus P, Fobker M, Seedorf U, Assmann G, Borchers T, Spener F. Phytanic acid is ligand and transcriptional activator of murine liver fatty acid binding protein. J Lipid Res. 1999; 40:708–714. [PubMed: 10191295]
21. Martin GG, Atshaves BP, Huang H, McIntosh AL, Williams BW, Pai PJ, Russell DH, Kier AB, Schroeder F. Hepatic phenotype of liver fatty acid binding protein (L-FABP) gene ablated mice. Am J Physiol. 2009; 297:G1053–G1065.
22. Martin GG, Atshaves BP, Landrock KK, Landrock D, Storey SM, Howles PN, Kier AB, Schroeder F. Ablating L-FABP in SCP-2/SCP-x null mice impairs bile acid metabolism and biliary HDL-cholesterol secretion. Am J Physiol Gastrointest and Liver Phys. 2014; 307:G1130–G1143.

23. Martin GG, Landrock D, Landrock KK, Howles PN, Atshaves BP, Kier AB, Schroeder F. Relative contributions of L-FABP, SCP-2/SCP-x, or both to hepatic biliary phenotype of female mice. Arch Biochem Biophys. 2015; 588:25–32. [PubMed: 26541319]
24. Chuang S, Velkov T, Horne J, Wielens J, Chalmers DK, Porter CJH, Scanlon MJ. Probing fibrate binding specificity of rat liver fatty acid binding protein. J Med Chem. 2009; 52:5344–5355. [PubMed: 19663428]
25. Chuang S, Velkov T, Horne J, Porter CJH, Scanlon MJ. Characterization of the drug binding specificity of rat liver fatty acid binding protein. J Med Chem. 2008; 51:3755–3764. [PubMed: 18533710]
26. Wolfrum C, Borchers T, Sacchettini JC, Spener F. Binding of fatty acids and perooxisome proliferators to orthologous fatty acid binding proteins from human, murine, and bovine liver. Biochemistry. 2000; 39:1469–1474. [PubMed: 10684629]
27. Di Pietro SM, Santome JA. Isolation, characterization, and binding properties of two rat liver fatty acid binding protein isoforms. Biochim Biophys Acta. 2000; 1478:186–200. [PubMed: 10825530]
28. Martin GG, McIntosh AL, Huang H, Gupta S, Atshaves BP, Kier AB, Schroeder F. Human liver fatty acid binding protein (L-FABP) T94A variant alters structure, stability, and interaction with fibrates. Biochemistry. 2013; 52:9347–9357. [PubMed: 24299557]
29. Mc Intosh AL, Huang H, Storey SM, Landrock K, Landrock D, Petrescu AD, Gupta S, Atshaves BP, Kier AB, Schroeder F. Human FABP1 T94A variant impacts fatty acid metabolism and PPARa activation in cultured human female hepatocytes. Am J Physiol Gastrointest and Liver Phys. 2014; 307:G164–G176.
30. Velkov T. Interactions between human liver fatty acid binding protein and peroxisome proliferator activated receptor drugs. PPAR Research. 2013; 2013:1–14.
31. Maatman RG, van Moerkerk HT, Nooren IM, van Zoelen EJ, Veerkamp JH. Expression of human liver fatty acid-binding protein in Escherichia coli and comparative analysis of its binding characteristics with muscle fatty acid-binding protein. Biochim Biophys Acta. 1994; 1214:1–10. [PubMed: 8068722]
32. Antonenkov VD, Sormunen RT, Ohlmeier S, Amery L, Fransen M. Localization of a portion of the liver isoform of fatty acid binding protein (L-FABP) to peroxisomes. Biochem J. 2006; 394:475–484. [PubMed: 16262600]
33. Gallegos AM, Atshaves BP, Storey SM, Starodub O, Petrescu AD, Huang H, McIntosh A, Martin G, Chao H, Kier AB, Schroeder F. Gene structure, intracellular localization, and functional roles of sterol carrier protein-2. Prog Lipid Res. 2001; 40:498–563. [PubMed: 11591437]
34. Martin GG, Hostetler HA, McIntosh AL, Tichy SE, Williams BJ, Russell DH, Berg JM, Spencer TA, Ball JA, Kier AB, Schroeder F. Structure and function of the sterol carrier protein-2 (SCP-2) N-terminal pre-sequence. Biochem. 2008; 47:5915–5934. [PubMed: 18465878]
35. Schroeder, F., Frolov, A., Schoer, J., Gallegos, A., Atshaves, BP., Stolowich, NJ., Scott, AI., Kier, AB. Intracellular Sterol Binding Proteins, Cholesterol Transport and Membrane Domains. In: Chang, TY., Freeman, DA., editors. Intracellular Cholesterol Trafficking. Kluwer Academic Publishers; Boston: 1998. p. 213-234.
36. Keller GA, Scallen TJ, Clarke D, Maher PA, Krisans SK, Singer SJ. Subcellular localization of sterol carrier protein-2 in rat hepatocytes: its primary localization to peroxisomes. J Cell Biol. 1989; 108:1353–1361. [PubMed: 2925789]
37. Wouters F, Bastiaens PI, Wirtz KW, Jovin TM. FRET microscopy demonstrates molecular association of non-specific lipid transfer protein (nsL-TP) with fatty acid oxidation enzymes. EMBO J. 1998; 17:7179–7189. [PubMed: 9857175]
38. Wanders RJ, Denis S, van Berkel E, Wouters F, Wirtz KWA, Seedorf U. Identification of the newly discovered 58 kDa peroxisomal thiolase SCP-x as the main thiolase involved in both pristanic acid and trihydroyxycholestanoic acid oxidation: Implications for peroxisomal beta-oxidation disorders. J Inher Metab Dis. 1998; 21:302–305. [PubMed: 9686381]
39. Wanders RJA, Denis S, Wouters F, Wirtz KWA, Seedorf U. Sterol carrier Protein X (SCPx) is a peroxisomal branched-chain b-ketothiolase specifically reacting with 3-Oxo-pristanoyl-CoA: A new, unique role for SCPx in branched-chain fatty acid metabolism in peroxisomes. Biochem Biophys Res Commun. 1997; 236:565–569. [PubMed: 9245689]

40. Seedorf U, Brysch P, Engel T, Schrage K, Assmann G. Sterol carrier protein X is peroxisomal 3-oxoacyl coenzyme A thiolase with intrinsic sterol carrier and lipid transfer activity. J Biol Chem. 1994; 269:21277–21283. [PubMed: 8063752]
41. Antonenkov VD, Van Veldhoven PP, Waelkens E, Mannaerts GP. Substrate specificities of 3-oxoacyl-CoA thiolase A and sterol carrier protein 2/3-oxoacyl-CoA thiolase purified from normal rat liver peroxisomes. J Biol Chem. 1997; 272:26023–26031. [PubMed: 9325339]
42. Antonenkov VD, Van Veldhoven PP, Mannaerts GP. Isolation and subunit composition of native sterol carrier protein-2/3-oxoacyl-coenzyme A thiolase from normal rat liver peroxisomes. Protein Exp Purif. 2000; 18:249–256.
43. Monnig G, Wiekowski J, Kirchhof P, Stypmann J, Plenz G, Fabritz L, Bruns HJ, Eckardt L, Assmann G, Haverkamp W, Breithardt G, Seedorf U. Phytanic acid accumulation is associated with conduction delay and sudden cardiac death in sterol carrier protein-2/sterol carrier protein-x deficient mice. J Cardiovasc Electrophysiol. 2004; 15:1310–1316. [PubMed: 15574183]
44. Seedorf, U. Functional Analysis of Sterol Carrier Protein-2 (SCP2) in SCP2 Knockout Mouse. In: Chang, TY., Freeman, DA., editors. Intracellular Cholesterol Trafficking. Kluwer Academic Publishers; Boston: 1998. p. 233-252.
45. Seedorf U, Raabe M, Ellinghaus P, Kannenberg F, Fobker M, Engel T, Denis S, Wouters F, Wirtz KWA, Wanders RJA, Maeda N, Assmann G. Defective peroxisomal catabolism of branched fatty acyl coenzyme A in mice lacking the sterol carrier protein-2/sterol carrier protein-x gene function. Genes and Development. 1998; 12:1189–1201. [PubMed: 9553048]
46. Atshaves BP, McIntosh AL, Landrock D, Payne HR, Mackie J, Maeda N, Ball JM, Schroeder F, Kier AB. Effect of SCP-x gene ablation on branched-chain fatty acid metabolism. Am J Physiol. 2007; 292:939–951.
47. Fuchs M, Hafer A, Muench C, Kannenberg F, Teichmann S, Scheibner J, Stange EF, Seedorf U. Disruption of the sterol carrier protein 2 gene in mice impairs biliary lipid and hepatic cholesterol metabolism. J Biol Chem. 2001; 276:48058–48065. [PubMed: 11673458]
48. Atshaves BP, Petrescu A, Starodub O, Roths J, Kier AB, Schroeder F. Expression and Intracellular Processing of the 58 kDa Sterol Carrier Protein 2/3-Oxoacyl-CoA Thiolase in Transfected Mouse L-cell Fibroblasts. J Lipid Res. 1999; 40:610–622. [PubMed: 10191285]
49. Storey SM, Atshaves BP, McIntosh AL, Landrock KK, Martin GG, Huang H, Johnson JD, Macfarlane RD, Kier AB, Schroeder F. Effect of sterol carrier protein-2 gene ablation on HDL-mediated cholesterol efflux from primary cultured mouse hepatocytes. Am J Physiol. 2010; 299:244–254.
50. Thigpen JE, Setchell KD, Ahlmark KB, Kocklear J, Spahr T, Caviness GF, Goelz MF, Haseman JK, Newbold RR, Forsythe DB. Phytoestrogen content of purified, open- and closed-formula laboratory animal diets. Lab An Science. 1999; 49:530–536.
51. Thigpen JE, Setchell KD, Goelz MF, Forsythe DB. The phytoestrogen content of rodent diets. Envron Health Persp. 1999; 107:A182–A183.
52. Ellinghaus P, Wolfrum C, Assmann G, Spener F, Seedorf U. Phytanic acid activates the peroxisome proliferator-activated receptor alpha (PPARalpha) in sterol carrier protein-2-/sterol carrier protein x-deficient mice. J Biol Chem. 1999; 274:2766–2772. [PubMed: 9915808]
53. Hanhoff T, Benjamin S, Borchers T, Spener F. Branched-chain fatty acids as activators of peroxisome proliferators. Eur J Lip Sci Technol. 2005; 107:716–729.
54. Atshaves BP, McIntosh AL, Kier AB, Schroeder F. High dietary fat exacerbates weight gain and obesity in female liver fatty acid binding protein gene ablated mice. Lipids. 2010; 45:97–110. [PubMed: 20035485]
55. Nagy TR, Clair AL. Precision and accuracy of dual-energy X-ray absorptiometry for in vivo body composition in mice. Obesity Research. 2000; 8:392–398. [PubMed: 10968731]
56. Livak KJ, Schmittgen TD. Analysis of relative gene expression data using real-time quantitative PCR and the 2^{-DDCT} method. Methods. 2001; 25:402–408. [PubMed: 11846609]
57. Klipsic D, Landrock D, Martin GG, McIntosh AL, Landrock KK, Mackie JT, Schroeder F, Kier AB. Impact of SCP-2/SCP-x gene ablation and dietary cholesterol on hepatic lipid accumulation. Am J Physiol Gastrointest and Liver Phys. 2015; 309:G387–G399.

58. Li T, Chiang JYL. Regulation of bile acid and cholesterol metabolism by PPARs. PPAR Research. 2009; 2009 Article ID 501739-15.

59. Repa JJ, Mangelsdorf DJ. The role of orphan nuclear receptors in the regulation of cholesterol homeostasis. Annu Rev Cell Dev Biol. 2000; 16:459–481. [PubMed: 11031244]

60. Trauner M, Boyer JL. Bile salt transporters: Molecular characterization, function, and regulation. Physiol Rev. 2003; 83:633–671. [PubMed: 12663868]

61. Jansen GA, Wanders RJA. Alpha Oxidation. Biochim Biophys Acta. 2006; 1763:1403–1412. [PubMed: 16934890]

62. Theil AC, Schutgens RB, Wanders RJ, Heymans HS. Clinical recognition of patients affected by a peroxisomal disorder: a retrospective study in 40 patients. Eur J Pediatrics. 1992; 151:117–120.

63. van den Brink DM, Wanders RJA. Phytanic acid: production from phytol, its breakdown and role in human disease. Cell Mol Life Sci. 2006; 63:1752–1765. [PubMed: 16799769]

64. Wanders RJA, Vreken P, Ferdinandusse S, Jansen GA, Waterham HR, van Roermund CW, van Grunsven EG. Peroxisomal fatty acid alpha and beta oxidation in humans: enzymology, peroxisomal metabolite transporters and peroxisomal diseases. Biochem Soc Trans. 2001; 29:250–267. [PubMed: 11356164]

65. Wanders RJA, Komen J, Ferdinandusse S. Phytanic acid metabolism in health and disease. Biochim Biophys Acta. 2011; 1811:498–507. [PubMed: 21683154]

66. Robitaille J, Brouillette C, Lemieux S, Perusse L, Gaudet D, Vohl MC. Plasma concentrations of apolipoprotein B are modulated by a gene-diet interaction effect between the L-FABP T94A polymorphism and dietary fat intake in French-Canadian men. Mol Gen and Metab. 2004; 82:296–303.

67. Fisher E, Weikert C, Klapper M, Lindner I, Mohlig M, Spranger J, Boeing H, Schrezenmeir J, Doring F. L-FABP T94A is associated with fasting triglycerides and LDL-cholesterol in women. Mol Gen and Metab. 2007; 91:278–284.

68. Weikert MO, Loeffelholz Cv, Roden M, Chandramouli V, Brehm A, Nowotny P, Osterhoff MA, Isken F, Spranger J, Landau BR, Pfeiffer A, Mohlig M. A Thr94Ala mutation in human liver fatty acid binding protein contributes to reduced hepatic glycogenolysis and blunted elevation of plasma glucsoe levels in lipid-exposed subjects. Am J Physiol Endocrinol Metab. 2007; 293:E1078–E1084. [PubMed: 17698986]

69. Yamada Y, Kato K, Oguri M, Yoshida T, Yokoi K, Watanabe S, Metoki N, Yoshida H, Satoh K, Ichihara S, Aoyagi Y, Yasunaga A, Park H, Tanaka M, Nozawa Y. Association of genetic variants with atherothrombotic cerebral infarction in Japanese individuals with metabolic syndrome. Int J Mol Med. 2008; 21:801–808. [PubMed: 18506375]

70. Bu L, Salto LM, De Leon KJ, De Leon M. Polymorphisms in fatty acid binding protein 5 show association with type 2 diabetes. Diabetes Res Clin Prac. 2011; 92:82–91.

71. Peng XE, Wu YL, Lu QQ, Ju ZJ, Lin X. Two genetic variants in FABP1 and susceptibility to non-alcoholic fatty liver disease in a Chinese population. Gene. 2012; 500:54–58. [PubMed: 22465531]

72. Mansego ML, Martinez F, Martinez-Larrad MT, Zabena C, Rojo G, Morcillo S, Soriguer F, Martin-Escudero JC, Serrano-Rios M, Redon J, Chaves FJ. Common variants of the liver fatty acid binding protein gene influence the risk of Type 2 Diabetes and insulin resistance in Spanish population. PLoS ONE. 2012; 7:e31853. [PubMed: 22396741]

73. Huang H, McIntosh AL, Martin GG, Landrock KK, Landrock D, Storey SM, Gupta S, Atshaves BP, Kier AB, Schroeder F. Human L-FABP T94A variant enhances cholesterol uptake. Biochim Biophys Acta. 2015; 1851:946–955. [PubMed: 25732850]

74. Brouillette C, Bose Y, Perusse L, Gaudet D, Vohl MC. Effect of liver fatty acid binding protein (FABP) T94A missense mutation on plasma lipoprotein responsiveness to treatment with fenofibrate. J Hum Gen. 2004; 49:424–432.

75. Tian Y, Li H, Wang S, Yan J, hen Z, i Z, eng H, Zhou H, Ouyang DS. Association of L-FABP T94A, MTP I128T polymorphisms and hyperlipidemia in Chinese subjects. Lipids. 2015; 50:275–282. [PubMed: 25663234]

76. Ferdinandusse S, Kostopoulos P, Denis S, Rusch R, Overmars H, Dillman U, Reith W, Haas D, Wanders RJA, Duran M, Marziniak M. Mutations in the gene encoding peroxisomal sterol carrier

protein-x (SCP-x) cause leukencephalopathy with dystonia and motor neuropathy. Am J Hum Genet. 2006; 78:1046–1052. [PubMed: 16685654]

77. Horvath R, Lewis-Smith D, Douroudis K, Duff J, et al. SCP2 mutations and neurodegeneration with brain iron accumulation. Neurology. 20165; 85:1909–1911.
78. Hostetler HA, McIntosh AL, Atshaves BP, Storey SM, Payne HR, Kier AB, Schroeder F. Liver type Fatty Acid Binding Protein (L-FABP) interacts with peroxisome proliferator activated receptor-a in cultured primary hepatocytes. J Lipid Res. 2009; 50:1663–1675. [PubMed: 19289416]
79. Huang H, Starodub O, McIntosh A, Atshaves BP, Woldegiorgis G, Kier AB, Schroeder F. Liver fatty acid binding protein colocalizes with peroxisome proliferator receptor alpha and enhances ligand distribution to nuclei of living cells. Biochemistry. 2004; 43:2484–2500. [PubMed: 14992586]
80. Martin GG, Atshaves BP, McIntosh AL, Mackie JT, Kier AB, Schroeder F. Liver fatty acid binding protein (L-FABP) gene ablation alters liver bile acid metabolism in male mice. Biochem J. 2005; 391:549–560. [PubMed: 15984932]
81. Martin GG, Atshaves BP, McIntosh AL, Mackie JT, Kier AB, Schroeder F. Liver fatty acid binding protein (L-FABP) gene ablation potentiates hepatic cholesterol accumulation in cholesterol-fed female mice. Am J Physiol. 2006; 290:G36–G48.
82. McIntosh AL, Atshaves BP, Hostetler HA, Huang H, Davis J, Lyuksyutova OI, Landrock D, Kier AB, Schroeder F. Liver type fatty acid binding protein (L-FABP) gene ablation reduces nuclear ligand distribution and peroxisome proliferator activated receptor-alpha activity in cultured primary hepatocytes. Arch Biochem Biophys. 2009; 485:160–173. [PubMed: 19285478]
83. Petrescu AD, McIntosh AL, Storey SM, Huang H, Martin GG, Landrock D, Kier AB, Schroeder F. High glucose potentiates liver fatty acid binding protein (L-FABP) mediated fibrate induction of PPARa in mouse hepatocytes. Biochim Biophys Acta. 2013; 1831:1412–1425. [PubMed: 23747828]
84. Petrescu AD, Huang H, Martin GG, McIntosh AL, Storey SM, Landrock D, Kier AB, Schroeder F. Impact of L-FABP and glucose on polyunsaturated fatty acid induction of PPARa regulated b-oxidative enzymes. Am J Physiol Gastrointest and Liver Phys. 2013; 304:G241–G256.
85. Atshaves BP, McIntosh AL, Payne HR, Gallegos AM, Landrock K, Maeda N, Kier AB, Schroeder F. Sterol carrier protein-2/sterol carrier protein-x gene ablation alters lipid raft domains in primary cultured mouse hepatocytes. J Lipid Res. 2007; 48:2193–2211. [PubMed: 17609524]
86. Murphy EJ, Prows DR, Jefferson JR, Schroeder F. Liver fatty acid binding protein expression in transfected fibroblasts stimulates fatty acid uptake and metabolism. Biochim Biophys Acta. 1996; 1301:191–198. [PubMed: 8664328]
87. Murphy EJ. L-FABP and I-FABP expression increase NBD-stearate uptake and cytoplasmic diffusion in L-cells. Am J Physiol. 1998; 275:G244–G249. [PubMed: 9688651]
88. Prows DR, Murphy EJ, Schroeder F. Intestinal and liver fatty acid binding proteins differentially affect fatty acid uptake and esterification in L-Cells. Lipids. 1995; 30:907–910. [PubMed: 8538377]
89. Hostetler HA, Lupas D, Tan Y, Dai J, Kelzer MS, Martin GG, Woldegiorgis G, Kier AB, Schroeder F. Acyl-CoA binding proteins interact with the acyl-CoA binding domain of mitochondrial carnitine palmitoyltransferase I. Mol Cell Biochem. 2011; 355:135–148. [PubMed: 21541677]
90. Woldegiorgis G, Bremer J, Shrago E. Substrate inhibition of carnitine palmitoyltransferase by palmitoyl-CoA and activation by phospholipids and proteins. Biochim Biophys Acta. 1985; 837:135–140. [PubMed: 4052442]
91. Jolly CA, Hubbell T, Behnke WD, Schroeder F. Fatty acid binding protein: stimulation of microsomal phosphatidic acid formation. Arch Biochem Biophys. 1997; 341:112–121. [PubMed: 9143360]
92. Schroeder F, Jolly CA, Cho TH, Frolov AA. Fatty acid binding protein isoforms: structure and function. Chem Phys Lipids. 1998; 92:1–25. [PubMed: 9631535]
93. Bordewick U, Heese M, Borchers T, Robenek H, Spener F. Compartmentation of hepatic fatty-acid-binding protein in liver cells and its effect on microsomal phosphatidic acid biosynthesis. Biol Chem Hoppe-Seyler. 1989; 370:229–238. [PubMed: 2653363]

94. Jefferson JR, Slotte JP, Nemecz G, Pastuszyn A, Scallen TJ, Schroeder F. Intracellular sterol distribution in transfected mouse L-cell fibroblasts expressing rat liver fatty acid binding protein. J Biol Chem. 1991; 266:5486–5496. [PubMed: 2005092]

95. Murphy EJ, Schroeder F. Sterol carrier protein-2 mediated cholesterol esterification in transfected L-cell fibroblasts. Biochimica Et Biophysica Acta. 1997; 1345:283–292. [PubMed: 9150248]

96. Atshaves BP, McIntosh AL, Martin GG, Landrock D, Payne HR, Bhuvanendran S, Landrock K, Lyuksyutova OI, Johnson JD, Macfarlane RD, Kier AB, Schroeder F. Overexpression of sterol carrier protein-2 differentially alters hepatic cholesterol accumulation in cholesterol-fed mice. J Lipid Res. 2009; 50:1429–1447. [PubMed: 19289417]

97. Zanlungo S, Amigo L, Mendoza H, Glick J, Rodriguez A, Kozarsky K, Miquel JF, Rigotti A, Nervi F. Overexpression of sterol carrier protein-2 in mice leads to increased hepatic cholesterol content and enterohepatic circulation of bile acids. Gastroenterology. 2000; 118:135 A1165.

98. Zanlungo S, Amigo L, Mendoza H, Miquel JF, Vio C, Glick JM, Rodriquez A, Kozarsky K, Quinones V, Rigotti A, Nervi F. Sterol carrier protein-2 gene transfer changes lipid metabolism and enterohepatic sterol circulation in mice. Gastroenterology. 2000; 119:1708–1719. [PubMed: 11113092]

Abbreviations

3αHSD	3alpha-hydroxysteroid reductase
ABCG5 or G8	ATP-binding cassette sub-family G member 5 or 8
ACAT2	acetyl-CoA acetyltransferase
ACBP	acyl-CoA-binding protein
ACC1	Acetyl-CoA carboxylase
AFABP	adipocyte fatty acid binding protein
AGPAT	1-acylglycerol-3-phosphate-O-acyltransferase
ALT	alanine aminotransferase
apoA1	apolipoprotein A-I
apoB	apolipoprotein B
AST	aspartate aminotransferase
B-FABP	brain fatty acid binding protein
β-OHB	β-hydroxybutyrate
BSEP	bile salt export pump
C	free cholesterol
CE	cholesteryl ester
COX4	cytochrome c oxidase subunit IV
CPT1a or 2	carnitine palmitoyltransferase 1a or 2
CRABP I	cellular retinoic acid binding protein 1

DEXA	dual-energy X-ray absorptiometry
DGAT	diacylglycerol acyltransferase
FASN	fatty acid synthase
FATP2, 4 and 5	fatty acid transport protein 2, 4 and 5
FTM	fat tissue mass
FxR	farnesoid x receptor
GAPDH	glyceraldehyde 3-phosphate dehydrogenase
GOT	glutamic oxaloacetic transaminase
GPAT/Gpam	glycerol-3-phosphate acyltransferase
GST	glutathione s-transferase
HDL-C	high density lipoprotein cholesterol
HMGCR	3-hydroxy-3-methylglutaryl-CoA reductase
HMGCS1, HMGCR	3-hydroxy-3-methylglutaryl-CoA synthase
I-FABP	intestinal fatty acid binding protein
LDL-R	low density lipoprotein receptor
L-FABP	liver fatty acid binding protein
LTM	lean tissue mass
LxR	liver x receptor
MDR	multidrug resistance protein
NEFA	non-esterified fatty acid
non-HDL-C	non-HDL cholesterol
NTCP	sodium-taurocholate cotransporting polypeptide
OATP1 or 2	organic anion-transporting polypeptide 1 or 2
PL	phospholipid
PPARα	peroxisome proliferator activated receptor alpha
qRT-PCR	quantitative real-time polymerase chain reaction
RxRα	retinoid x receptor α
SCP2	sterol carrier protein 2
SCPx	sterol carrier protein x

SEM	standard error of the mean
SR-B1	scavenger receptor class B member 1
SREBP1 and 2	sterol regulatory element-binding protein 1 and 2
TC	total cholesterol
TG	triglyceride/triacylglycerol
TKO	L-FABP/SCP2/SCPx null
TLC	thin layer chromatography
WT	wild-type

Highlights

- FABP1/SCP2/SCPx ablation (TKO) impacts liver lipids in phytol-fed female mice.
- TKO increased liver phospholipid and enzymes of phospholipid synthetic pathway.
- TKO reduced liver triacylglycerol and enzymes of triacylglycerol synthetic pathway.
- TKO exacerbated dietary phytol-induced whole body weight loss, especially lean tissue mass.
- TKO helps resolve contributions of FABP1 and SCP2/SCPx genes in female mice.

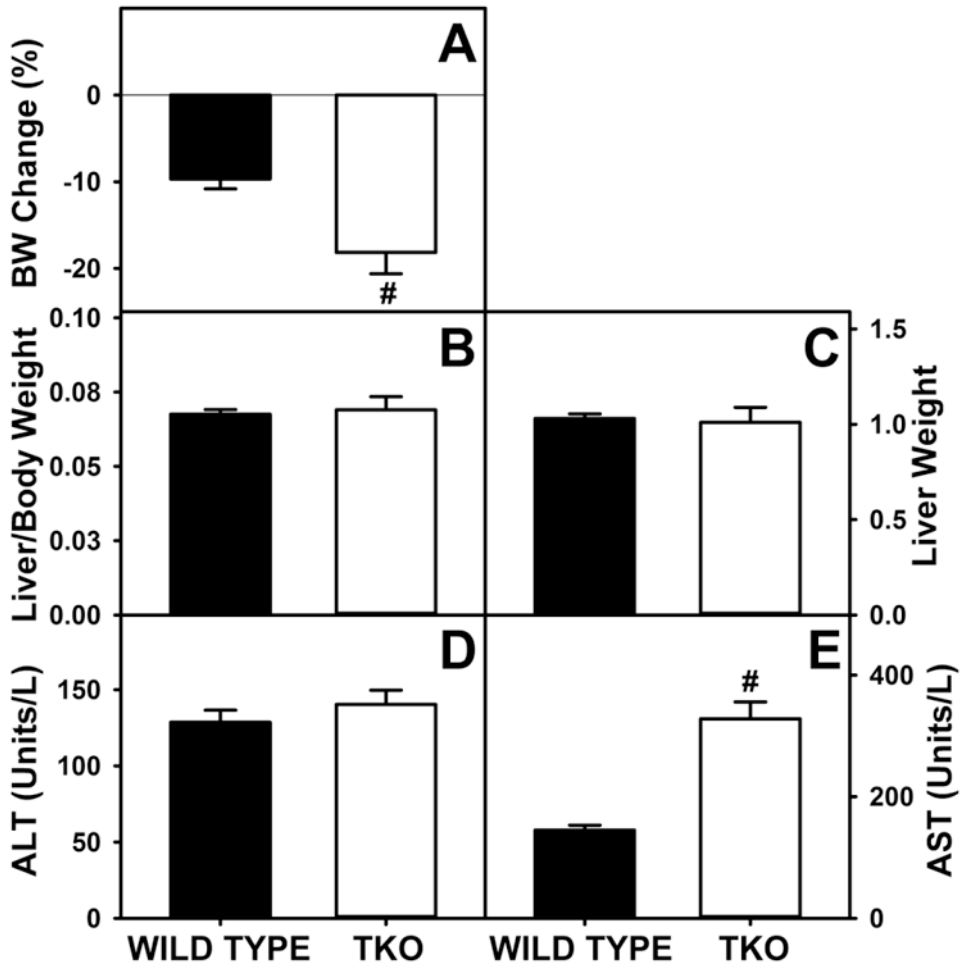

Figure 1. Body Weight, Liver Weight and Serum AST and ALT

Percent change in body weight (A), ratio of body weight per gram of liver weight (B), liver weight (C) and serum levels of ALT (D) and AST (E) were determined for wild-type (WT) and L-FABP/SCP2/SCPx gene ablated (TKO) female mice fed a 0.5% phytol diet as described in Experimental Procedures. Means +/- SE; n= 8 animals/group; $^{\#}p < 0.05$ between phytol-fed WT versus phytol-fed TKO mice.

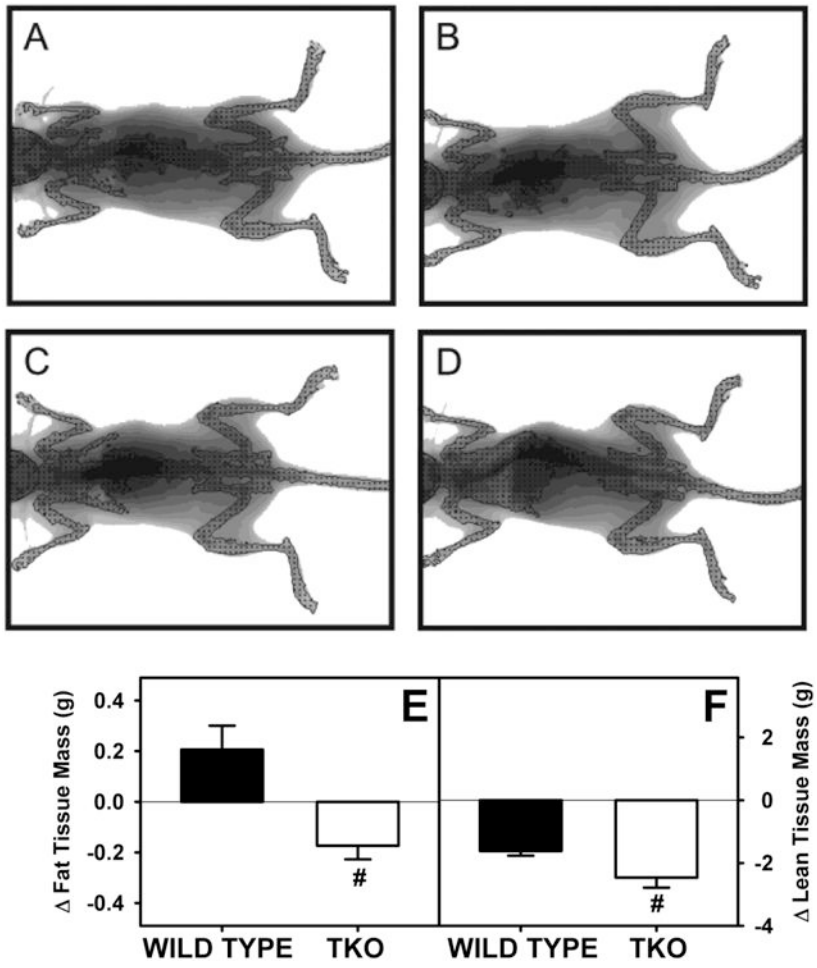

Figure 2. Body Composition of Fat Tissue Mass and Lean Tissue Mass

Whole body phenotype of WT and TKO mice fed a 0.5% phytol diet was determined by Lunar PIXImus dual-energy x-ray absorptiometry (DEXA). DEXA resolved whole body fat tissue mass (FTM) and lean tissue mass (LTM). A and B are representative images of control diet fed WT and TKO mice at the end of the study, respectively. C and D are representative images of phytol diet fed WT and TKO mice at the end of the study, respectively. The change in FTM (E) and LTM (F) was determined for 8 mice per group. Means +/- SE; n= 8 animals per group; $^{\#}p < 0.05$ between phytol-fed WT versus phytol-fed TKO mice.

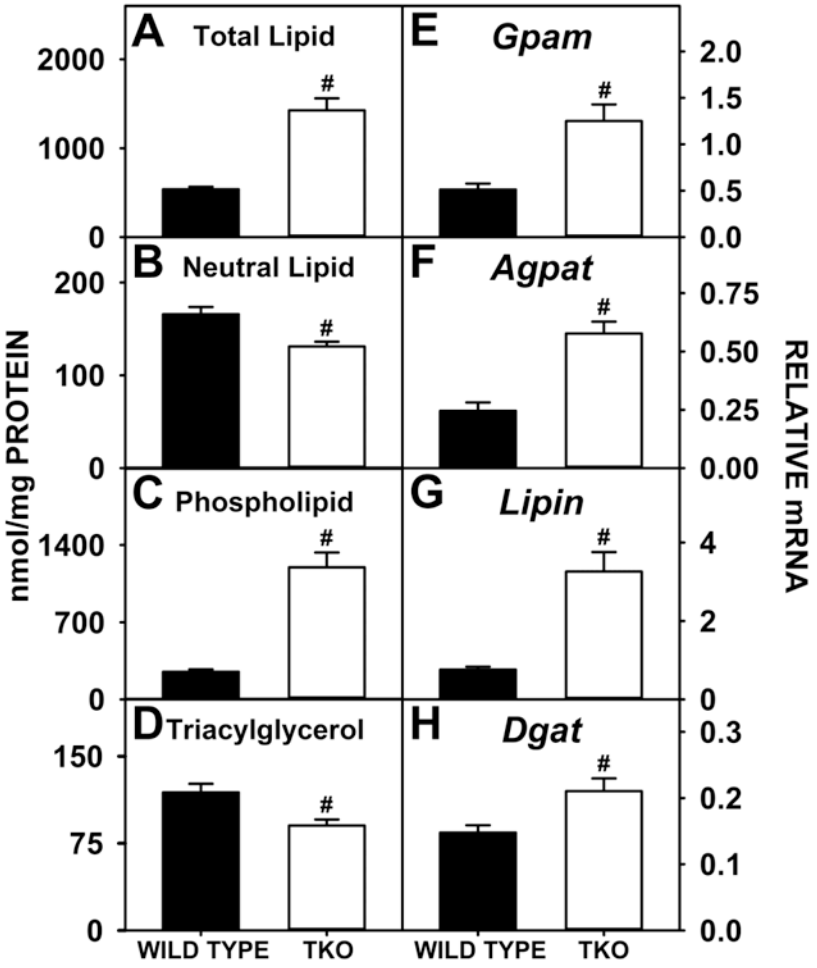

Figure 3. Hepatic Lipid Levels and Expression of Key Proteins in Glyceride Synthesis

WT and TKO mice were fed a 0.5% phytol diet as described in Experimental Procedures. Levels of total hepatic lipid (A), hepatic neutral lipid (B), hepatic phospholipid (C) and hepatic triacylglycerol (D) were measured and qRT-PCR was performed to measure the expression of *Gpam* (E), *Agpat2* (F), *Lipin2* (G) and *Dgat2* (H) as in Experimental Procedures. Means +/- SE; n= 8 animals per group; $^{\#}p < 0.05$ between phytol-fed WT versus phytol-fed TKO mice.

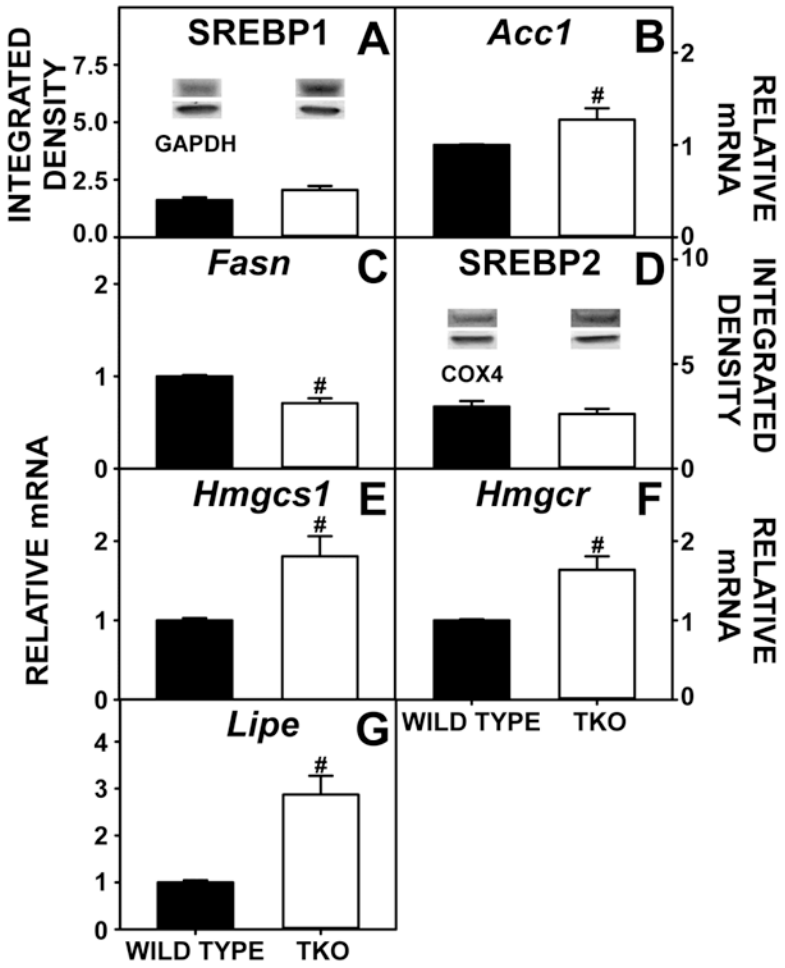

Figure 4. Hepatic Expression of SREBPs and Target Genes in *de novo* Fatty Acid and Cholesterol Synthesis

Livers from WT and TKO mice fed a 0.5% diet phytol diet were examined by western blotting as in Experimental Procedures to measure relative hepatic protein levels of SREBP1 (A) and SREBP2 (D). The housekeeping gene GADPH or COX4 was used as a loading control to normalize protein expression for SREBP1 and SREBP2, respectively. Inset in Panels A and D show representative western blots of relative protein expression in each mouse group. qRT-PCR was performed to determine relative transcription of SREBP1 target genes *Acc1* (C) and *Fasn* (D), transcription of SREBP2 target genes *Hmgcs1* (E) and *Hmgcr* (F) and *Lipe* (G) also as in Experimental Procedures. 18S rRNA was used to normalize mRNA expression levels. Means +/- SE; n= 8 animals per group; $^{\#}p < 0.05$ between phytol-fed WT versus phytol-fed TKO mice.

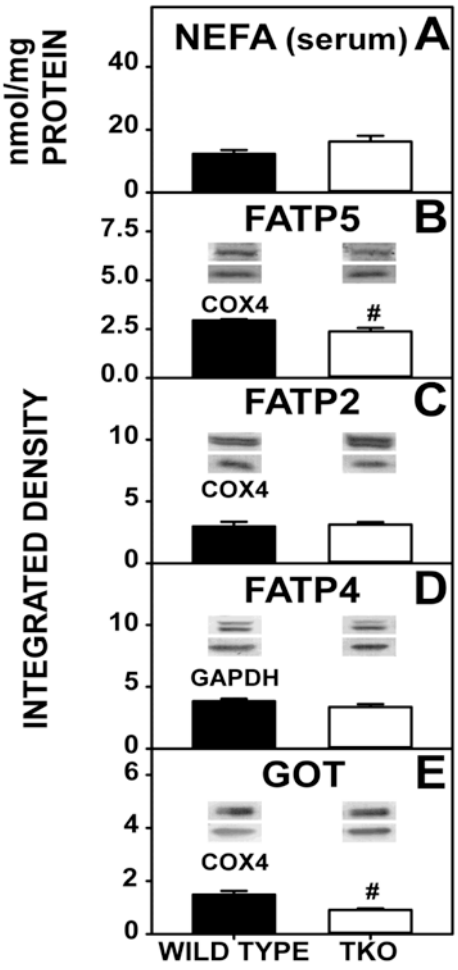

Figure 5. Fatty Acid Uptake and Expression of Membrane Fatty Acid Transport Proteins

WT and TKO mice were fed a 0.5% phytol diet as described in Experimental Procedures. Serum NEFA was measured (A) and western blotting was performed to measure the expression of FATP5 (B), FATP2 (C), FATP4 (D), and GOT (E) as in Experimental Procedures. The housekeeping gene COX4 was used as a loading control to normalize FATP5, FATP2 and GOT expression. GADPH was used as a loading control to normalize FATP4 expression. Insets in Panels B-E show representative western blots of relative protein expression in each mouse group. Means +/- SE; n= 8 animals per group; $^{\#}p < 0.05$ between phytol-fed WT versus phytol-fed TKO mice.

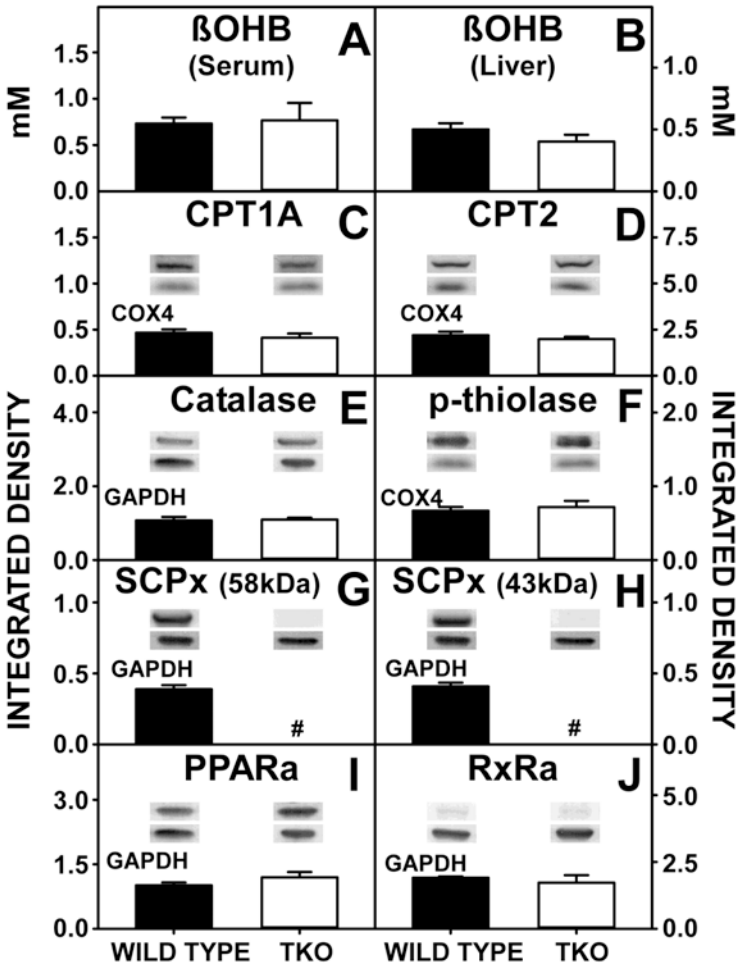

Figure 6. Fatty Acid Oxidation

WT and TKO mice were fed a 0.5% phytol diet as described in Experimental Procedures. Serum (A) and liver (B) concentrations of β-hydroxybutyrate (β-OHB) were determined and western blotting was performed to measure the hepatic expression of CPT1A (C), CPT2 (D), catalase (E), p-thiolase (F), SCPx (G and H), PPARα (I) and RxRα (J) as described in Experimental Procedures. The housekeeping gene COX4 was used as a loading control to normalize CPT1A, CPT2 and p-thiolase expression. GADPH was used as a loading control to normalize catalase, SCPx, PPARα and RxRα expression. Inset in Panels C-J show representative western blots of relative protein expression in each mouse group. Means +/- SE; n= 8 animals per group; $^{\#}p < 0.05$ between phytol-fed WT versus phytol-fed TKO mice.

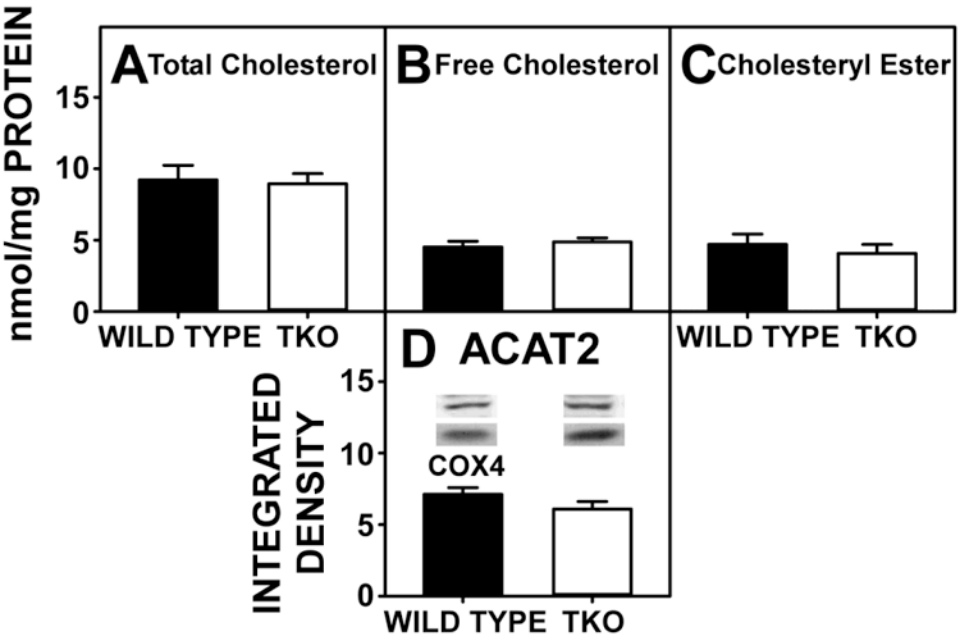

Figure 7. Expression of Proteins in the Cholesteryl Ester Synthesis/Hydrolysis Cycle

WT and TKO mice were fed a 0.5% phytol diet as described in Experimental Procedures. Levels of total hepatic cholesterol (A), hepatic free cholesterol (B), and hepatic cholesteryl ester (C) and were assayed; western blots were performed to measure the expression of ACAT2 as described in Experimental Procedures. The housekeeping gene COX4 was used as a loading control to normalize protein expression. Inset in Panel D shows representative western blotting of relative protein expression in each mouse group. Means +/- SE; n= 8 animals per group; $^{\#}p < 0.05$ between phytol-fed WT versus phytol-fed TKO mice.

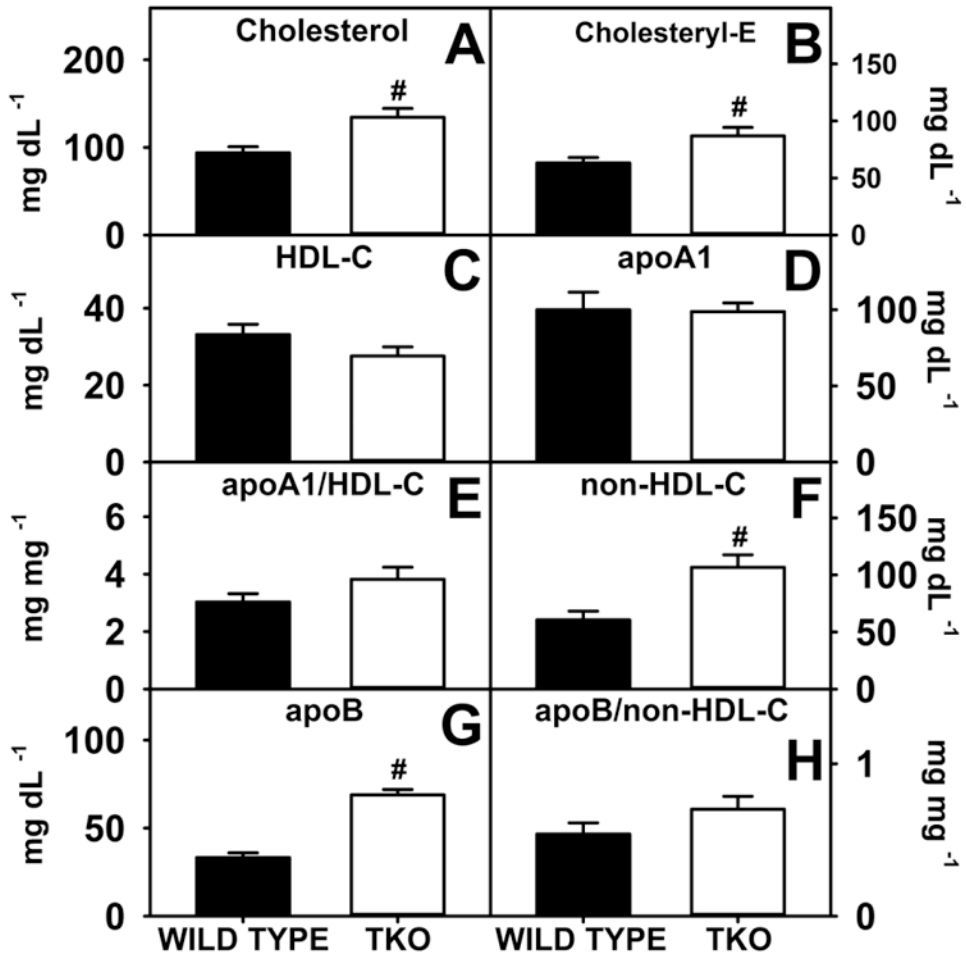

Figure 8. Serum Lipid and Lipoprotein Levels

WT and TKO mice were fed a 0.5% phytol diet as described in Experimental Procedures. Serum levels of free cholesterol (A), cholesteryl ester (B), HDL cholesterol (C), apoA1 (D), non-HDL-C (F) and apoB (G) were measured and the apoA1/HDL-C (E) and apoB/non-HDL-C (H) ratios were calculated as described in Experimental Procedures. Means +/- SE; n= 8 animals per group; $^{\#}p < 0.05$ between phytol-fed WT versus phytol-fed TKO mice.

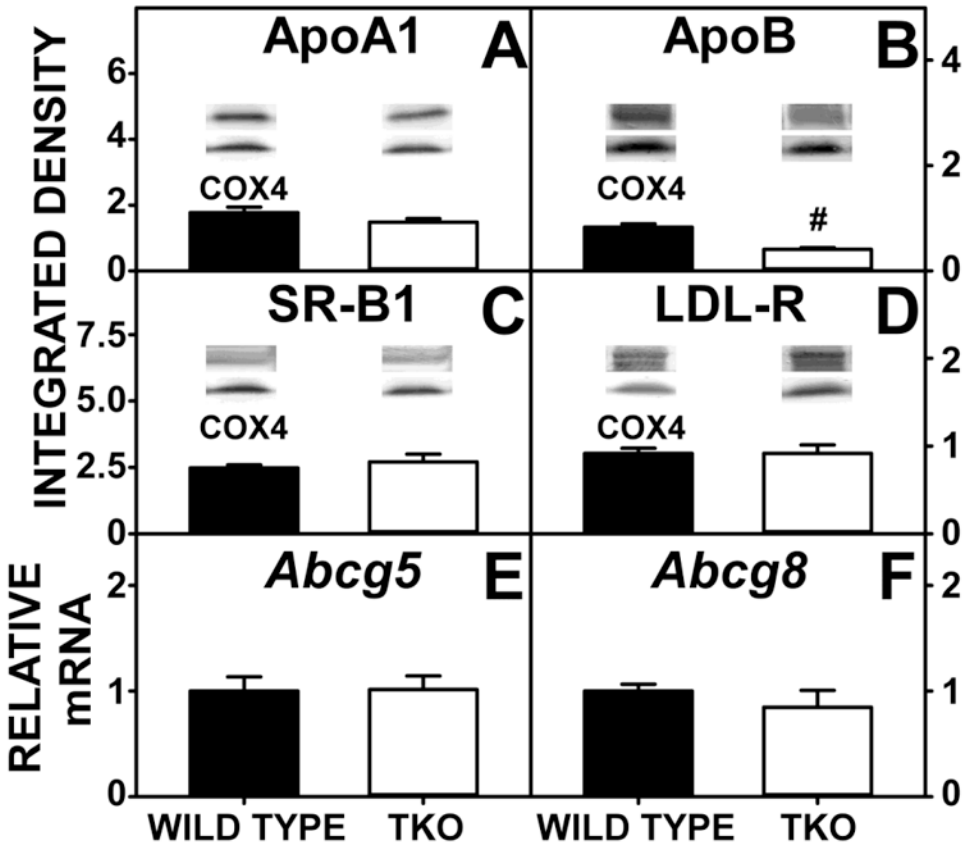

Figure 9. Expression of Hepatic Proteins Involved in Cholesterol Uptake, Efflux and Biliary Secretion

WT and TKO mice were fed a 0.5% phytol diet as described in Experimental Procedures. Levels of hepatic apoA1 (A), apoB (B), SR-B1 (C) and LDL-R (D were determined by western blotting as in Experimental Procedures. The housekeeping gene COX4 was used as a loading control to normalize protein expression. Inset in Panels A-D show representative western blots of relative protein expression in each mouse group. qRT-PCR was performed to determine relative transcription of *Abcg5* (E) and *Abcg8* (F) as in Experimental Procedures. 18S rRNA was used to normalize mRNA expression levels. Means +/- SE; n= 8 animals per group; $^{\#}p < 0.05$ between phytol-fed WT versus phytol-fed TKO.

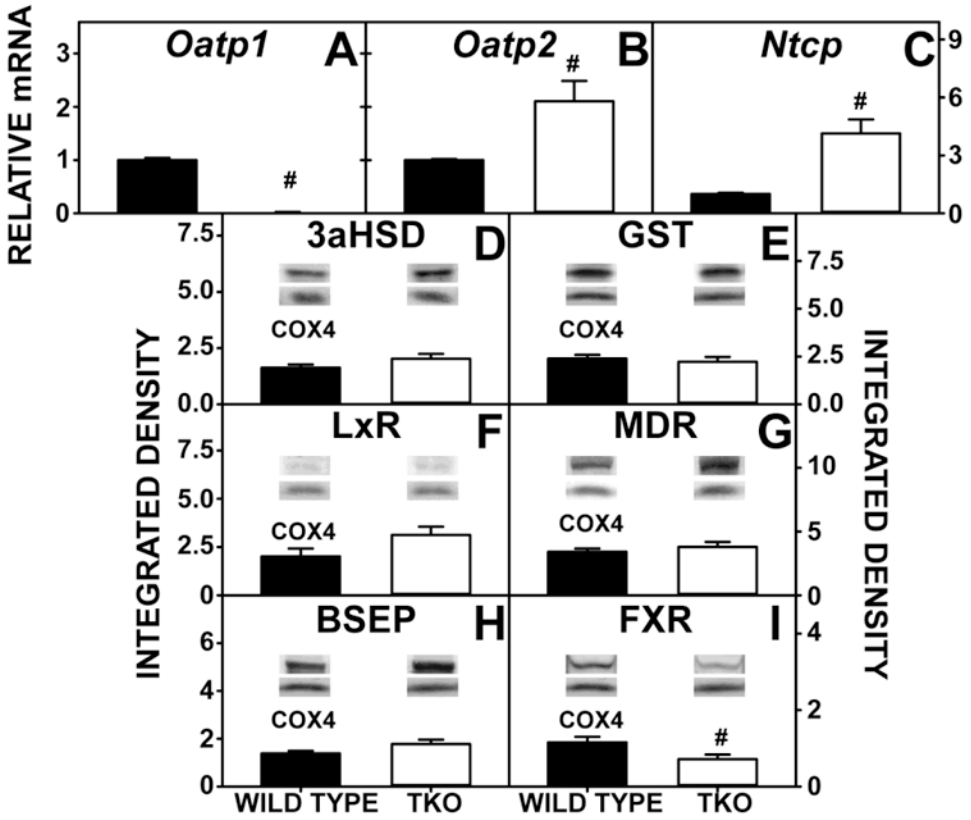

Figure 10. Hepatic Expression of Proteins for Bile Acid Transport

WT and TKO mice were fed a 0.5% phytol diet as described in Experimental Procedures. qRT-PCR was performed to measure the expression of *Oatp1* (A), *Oatp2* (B) and *Ntcp* (C). 18S rRNA was used to normalize mRNA expression levels. Western blotting was performed to measure the expression of 3αHSD (D), GST (E), LxR (F), MDR (G), BSEP (H), and FxR (I). The housekeeping gene COX4 was used as a loading control to normalize protein expression. Inset in Panels D-I show representative western blots of relative protein expression in each mouse group. Means +/- SE; n= 8 animals per group; $^{\#}p < 0.05$ between phytol-fed WT versus phytol-fed TKO mice.

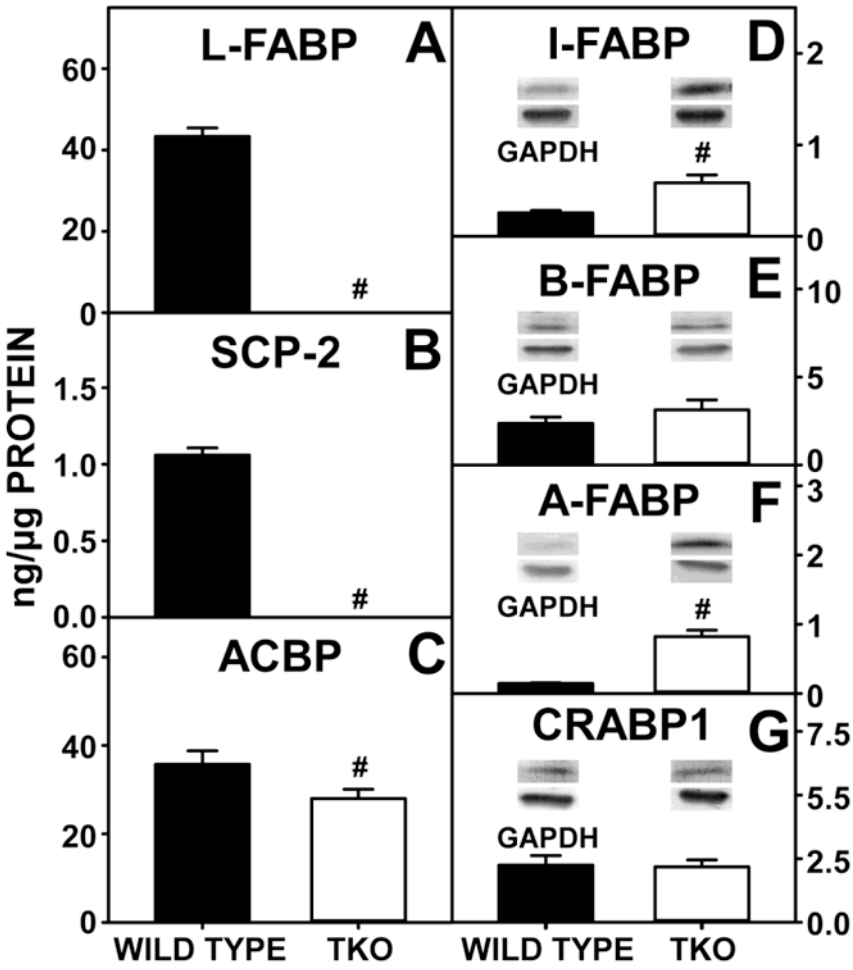

Figure 11. Lipid Binding and Transport Proteins

WT and TKO mice were fed a 0.5% phytol diet as described in Experimental Procedures. Quantitative western blotting was performed to measure the expression of L-FABP (A), SCP2 (B) and ACBP (C) as described in Experimental Procedures. Additional western blotting was performed to measure the relative expression of I-FABP (D), B-FABP (E), A-FABP (F) and CRABP-1 (G). The housekeeping gene GADPH was used as a loading control to normalize protein expression. Inset in Panels D-G show representative western blots of relative protein expression in each mouse group. Means +/- SE; n= 8 animals per group; $^{\#}p < 0.05$ between phytol-fed WT versus phytol-fed TKO mice.